

University of Belgrade
Faculty of Technology and Metallurgy

Gamal Ali Mohamed Lazouzi

**Synthesis and characterization of modified
acrylate and alumina particles composite with
improved toughness for prosthetics application**

Doctoral dissertation

Belgrade, 2018

Univerzitet u Beogradu
Tehnološko-metalurški fakultet

Gamal Ali Mohamed Lazouzi

**Sinteza i karakterizacija kompozita sa
poboljšanom žilavošću na bazi modifikovanog
akrilata i aluminijum-oksidnih čestica za
primenu u protetici**

Doktorska disertacija

Beograd, 2018

Thesis advisors

Prof. Dr Radmila Jančić Heinemann, full professor, University of Belgrade, Faculty of Technology and Metallurgy

Prof. Dr Tamara Perić, assistant professor, University of Belgrade, Faculty of Stomatology

Jury

.....
Prof. dr Pavle Spasojević, associate professor,
University of Kragujevac, Faculty of Technical
Sciences Čačak.

.....
Dr Marija Vuksanović, research associate,
Inovation Center, Faculty of Technology and
Metallurgy

.....
Prof. dr Vesna Radojević, full professor,
University of Belgrade, Faculty of Technology
and Metallurgy

Candidate Gamal Lazouzi: _____

Date of defence _____

Acknowledgment

This thesis has been done in the department of materials science at the faculty of technology and metallurgy in Belgrade. First of all I would like to thank *Allah (god)* who gives me the life to be here, having great moments at the Faculty of Technology and Metallurgy, as well as getting a good idea about new culture and friendly people. Secondly, I would offer a special thanks to my parents for giving a strong support and all family member and friends, and to share these happy moments with my wife and my children who were with me during my stay in Serbia, and never felt home sick because of them. I would honor to have the chance to meet Prof Radoslav Aleksić who passed away but who gave me the basics of my knowledge in materials science and the approach in research. In addition, I would like to express my deep gratitude to my supervisors for their patient guidance, encouragement, their advices and aid in making this thesis completed and the member of the jury for careful reading. The experimental work was done in the laboratory at the department so my grateful thanks are also extended to Dr Natasa Tomić that her aid was crucial for completion of experimental part of this thesis. I would like to express my very great appreciate to Dr Marija Vukasnović and Dr Pavle Spasojević for the consultation in the thesis writing.

Finally I would to thank all the people who are involved in this work and the staff at student office who helped me during my study in the faculty and specific thank to Prof. Dr Nenad Radović who helped me a lot.

Summary

Synthesis and characterization of modified acrylate and alumina particles composite with improved toughness for prosthetics application

Key words: composite, PMMA, mechanical properties,

Scientific field: technological engineering

Dental materials have special requirements concerning their behavior in exploitation. Polymethyl methacrylate has been used in dentistry for various applications. It is interesting to improve mechanical properties of the material by addition of ceramic nanoparticles. In this paper, the addition of commercial spherical alumina particles as well as the ferrous-doped alumina nano particles influences mechanical properties of the obtained composite were assessed.

It has been proven that addition of spherical alumina nano particles improves flexural strength as well as the modulus of elasticity of the composite. It was shown that addition of 5 wt. % of spherical nano particles improves the mechanical properties of the composite. The addition of spherical nano particles also improves the impact strength of the obtained composite.

Addition of the ferrous-doped alumina nanoparticles improves the modulus of elasticity of the obtained composite and it was shown that the addition of 3 wt. % of those fillers gives the best result concerning the modulus of elasticity as well as resistance to impact compared to pure PMMA.

Key words: composite materials, PMMA, mechanical properties

Scientific field: Technological engineering

Narrow scientific field: materials engineering

Sažetak

Sinteza i karakterizacija kompozita sa poboljšanom žilavošću na bazi modifikovanog akrilata i aluminijum-oksidnih čestica za primenu u protetici

Dentalni materijali imaju posebne zahteve u vezi sa ponašanjem u uslovima eksploatacije. Poli (metil metakrilat) predstavlja jedan od često korišćenih materijala u protetici. Od interesa je da se poboljšaju mehanička svojstva polimerne matrice dodatkom ojačanja u obliku keramičkih nanočestica. Pokazalo se da se dodavanjem veoma malih količina čestica u materijal dobijaju bitno poboljšana mehanička svojstva. U okviru ovog rada ispitivano je kako dodatak komercijalnih nano čestica aluminijum-oksida utiče na mehanička svojstva dobijenog kompozitnog materijala i biće ispitana metodom udara kontrolisane energije. U prethodnim istraživanjima pokazalo se da dodatak do 5 mas. % nano čestičnog punioca bitno poboljšava mehanička svojstva. Dobijeni rezultati ukazali su na mogućnost korišćenja ovih materijala u uslovima izloženosti udaru, kao i na količinu ojačanja koja se može dodati kako bi se ostvarila optimizacija svojstava i načina pripreme kompozitnog materijala.

Pokazano je da dodatak aluminijum oksidnih sferičnih nanočestica dopiranih gvožđe oksidom poboljšava mehanička svojstva materijala u odnosu na čist PMMA. Sa druge strane prilikom ispitivanja udarom, najbolje rezultate pokazuju kompoziti kod kojih je ojačanje od aluminijum oksidnih čestica.

Ključne reči: kompozit, PMMA, mehanička svojstva

Naučna oblast: tehnološko inženjerstvo

Uža naučna oblast: inženjerstvo materijala

CONTENTS

Introduction	1
1 Polymethyl methacrylate PMMA	2
1.1 Production and uses of PMMA.....	2
1.2 Uses of PMMA in medicine and dentistry.....	4
1.3 Biocompatibility of PMMA.....	8
1.4 Itaconic acid and the uses of polyitaconate	8
1.5 Introducing itaconate into PMMA in order to obtain better biocompatibility.....	9
2 Composite materials.....	13
2.1 Classification of composite materials	14
2.2 Particle-reinforced composites	17
3 Nanosized reinforcement particles in polymer matrix composites	19
3.1 Alumina nano particles	19
3.2 Alumina nanoparticles reinforced PMMA	22
4 Characterization methods.....	24
4.1 Particle size and morphology analysis.....	24
4.2 Crystal structure analysis	24
4.3 FT-IR structure analysis.....	25
4.4 Mechanical testing	25
4.4.1 Microhardness measurements	25
4.4.2 Toughness measurements	26

4.4.3	Residual monomer determination.....	27
5	Experimental part	32
5.1.1	Materials and sample preparation.....	32
5.1.2	Specimen preparation	33
6	RESULTS AND DISCUSSION	35
6.1	Particle size distribution of synthesized alumina particles	35
6.2	Particle morphology obtained from FE-SEM analysis	36
6.3	Microstructure of the particles and PMMA composites	38
6.4	The XRD analysis of alumina particles crystal structure.....	42
6.5	Structure characterization via FTIR spectroscopy for alumina based particles at different temperatures	45
6.6	Structure characterization via FTIR spectroscopy for PMMA/DMI/Al ₂ O ₃ composites	45
6.7	Micro hardness measurements of PMMA composites	50
6.8	Tensile testing for PMMA composite.....	52
6.9	Mechanical properties of dental PMMA/DMI/Al ₂ O ₃ composites.....	54
6.9.1	Tensile testing of PMMA/DMI/Al ₂ O ₃	55
6.9.2	Toughness testing of PMMA/DMI/Al ₂ O ₃	56
6.9.3	Micro Vickers hardness of PMMA/DMI/Al ₂ O ₃	57
6.9.4	Controlled energy impact testing.....	59
6.10	Residual monomer determination	65
6.11	The 3 point bending test.....	67
7	CONCLUSION	73
8	REFERENCE	76

INTRODUCTION

The composite materials are important part of our everyday life and they are present from ancient times at first as natural composite materials, but very early in the human development, they were produced artificially in order to achieve better materials properties. Today, the composite materials have new applications and among most interesting ones is the one as a biomaterial. Materials that are used inside the body or in close contact to the body must meet some special demands such as to be nontoxic, to be biocompatible and to last the time they are designed to fulfill the special aspects of the use.

Polymethyl methacrylate has been used in dentistry and medicine for a long time. The main demand of this material is to enable good material properties with keeping the good mechanical properties and remaining nontoxic. One of the possible disadvantages is to polymerize the monomer until there is the less possible amount of monomer resting in the specimen. It has been found that the addition of small amounts of itaconate in the form of ethyl-itaconate can diminish the quantity of the monomer that rests on the material and in this way to increase the biocompatibility of the material. On the other hand, this addition reduces the mechanical properties of the material.

Addition of small amount of nanoparticles creates the composite material that has improved mechanical properties. Alumina nanoparticles are excellent candidate to improve mechanical properties of the material. The improvement of the modulus of elasticity and resistance to impact can be achieved in those composite materials. The purpose of this work was to test the possibility to improve mechanical properties of the matrix that is more biocompatible, and has less residual monomer in the structure.

Composite material consisting of a PMMA – itaconate copolymer was used as a matrix and the alumina nanoparticles were used as filler in order to improve mechanical properties.

1 POLYMETHYL METHACRYLATE PMMA

Polymethyl methacrylate was discovered in the early 1930s by British chemists Rowland Hill [1] and John Crawford at Imperial Chemical Industries (ICI) in England. ICI registered the product under the trademark Perspex. About the same time, chemist and industrialist Otto Röhm [2] of Rohm and Haas AG in Germany attempted to produce safety glass by polymerizing a methyl methacrylate between two layers of glass. The polymer separated from the glass as a clear plastic sheet, which Röhm gave the trademarked name Plexiglas. Both Perspex and Plexiglas were commercialized in the late 1930s. In the United States, E.I. du Pont de Nemours & Company subsequently introduced its own product under the trademark Lucite. The first major application of the new plastic took place during World War II, when PMMA was made into aircraft windows and bubble canopies for gun turrets. Civilian applications followed after the war.

1.1 PRODUCTION AND USES OF PMMA

Polymethyl methacrylate (PMMA), a polymer produced from the polymerization of methyl methacrylate. The result is a transparent and a rigid plastic material, PMMA is often used in applications where transparency is important such as shatterproof windows, skylights, architecture, design objects, and aircraft canopies. The usual name for this product is the trademarks Plexiglas, Lucite and Perspex.

PMMA, an ester of methacrylic acid ($\text{CH}_2=\text{C}[\text{CH}_3]\text{CO}_2\text{H}$), belonging to the family of acrylic resins. Usually is produced from propylene resulting from distillation on of crude oil, especially of the lighter fractions. Propylene and benzene are reacted together to form cumene, or isopropyl benzene; the cumene is oxidized to cumene hydro peroxide, which is treated with acid to form acetone; the acetone is in turn converted in a three-step process for methyl methacrylate ($\text{CH}_2=\text{C}[\text{CH}_3]\text{CO}_2\text{CH}_3$), a flammable liquid. Methyl methacrylate, in bulk liquid form or suspended as fine droplets in water, is polymerized under the influence

of free-radical initiators to form solid PMMA. The structure of the polymer-repeating unit is presented in

Figure 1.

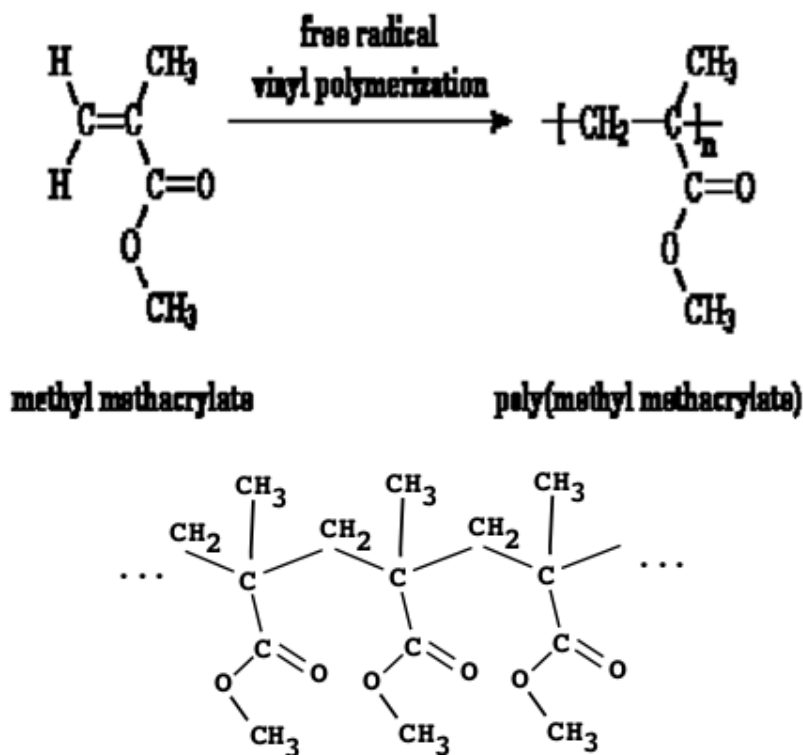


Figure 1 The structural formula representation of MMA monomer and the representation of the polymerized monomer.

The presence of the pendant methyl (CH₃) groups prevents the polymer chains from packing closely in a crystalline fashion and from rotating freely around the carbon-carbon bonds. As a result, PMMA is a tough and rigid plastic. In addition, it has an almost perfect transmission of visible light and because it retains these properties over years of exposure to ultraviolet light and weather, it is an ideal substitute for glass. A most successful application is internally lighted signs for advertising and directions. PMMA is also employed in domed skylights, swimming pool enclosures, aircraft canopies, instrument panels, and luminous ceilings. For these applications, the plastic is drawn into sheets that are machined or thermoformed, but it

is also injection-molded into automobile lenses and lighting-fixture covers. Because PMMA displays the unusual property of keeping a beam of light reflected within its surfaces, it is frequently made into optical fibers for signal transmission on small distances and endoscopy. Polymethyl methacrylate is used as a substitute for transparent glass and dielectric films [3], acrylic paints [4], micro-cell foam [5]. However, biomedicine represents the most attractive application area where this material is used to create denture bases [6], contact lenses, bone cement [7], inhalers [8]. The schematic representation of uses of PMMA in building and construction, optics, automotive, healthcare medical dental applications is illustrated in Figure 2.

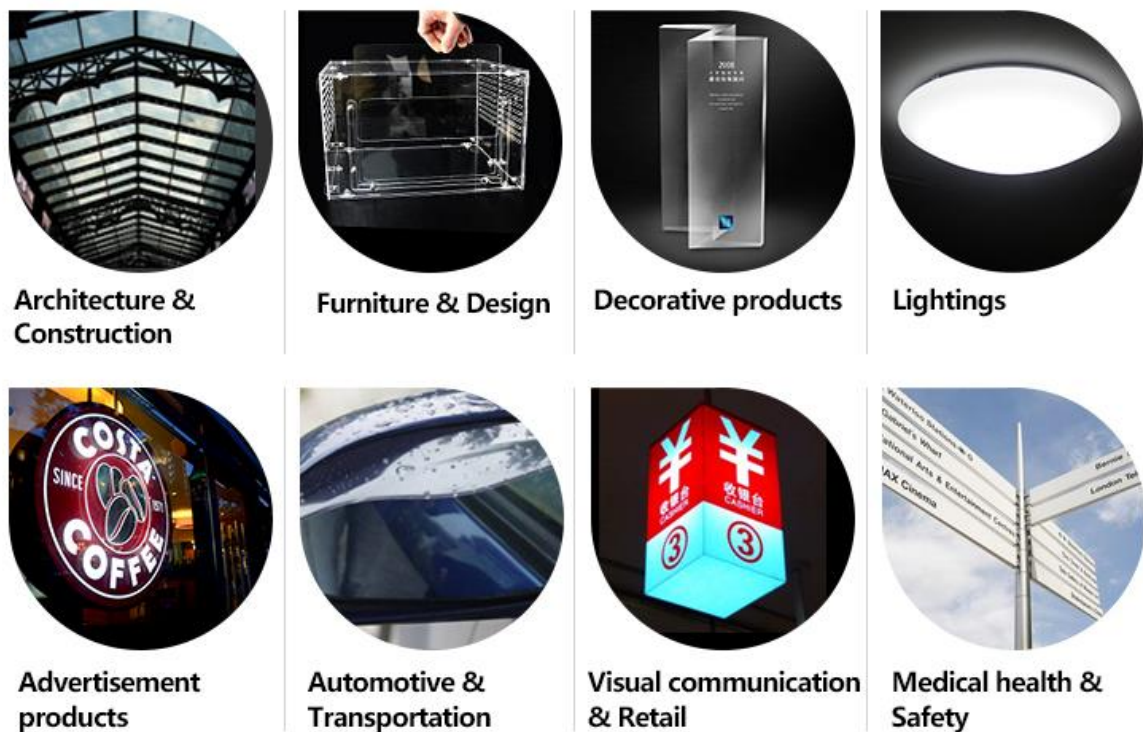


Figure 2 The schematic representation of several uses of PMMA [9].

1.2 USES OF PMMA IN MEDICINE AND DENTISTRY

The first use of polymethyl methacrylate (PMMA) as a dental device was for the fabrication of complete denture bases. Its qualities of biocompatibility, reliability, relative ease of

manipulation, and low toxicity were soon seized upon and incorporated by many different medical specialties. PMMA has been used for (a) bone cements; (b) contact and intraocular lens; (c) screw fixation in bone; (d) filler for bone cavities and skull defects; and (e) vertebrae stabilization in osteoporotic patients. The many uses of PMMA in the field of medicine will be the focus of this review, with particular attention paid to assessing its physical properties, advantages, disadvantages, and complications. Although numerous new alloplastic materials show promise, the versatility and reliability of PMMA cause it to remain a popular and frequently used material [10].

Polymethyl methacrylate (PMMA) also known as bone cement has been a frequently used material for medical applications. PMMA reveals typical brittle material behavior with high compression (83 MPa) by rather low-tension stress (35 MPa). No significant difference was measured between dry stored and 37 °C saline solution stored specimens regarding tensile, compression and flexural properties. As bone cement can be considered as a viscoelastic material, additional tests under varied strain rates revealed an increasing Young's modulus and ultimate strength of PMMA (Palacos R) with increasing strain rate. To evaluate long-term load-cycling behaviour an S-N curve was determined [11]. Some producer-defined properties of PMMA are given in

Table 1.

Table 1 Polymethyl methacrylate Properties [12].

Property	Value	Property	Value
Polymethyl methacrylate	Dimensional Stability	Fire Performances	
Coefficient of Linear Thermal Expansion	5 - 9 10^{-5} /°C	Fire Resistance (LOI)	19 - 20 %
Shrinkage	0.2 – 0.8 %	Flammability UL94	HB
Water Absorption 24 hours	0.1 – 0.4 %	Polymethyl methacrylate Optical Properties	
Polymethyl methacrylate	Electrical Properties	Haze	1 - 96 %
Dielectric Constant	2 - 5	Transparency (% Visible Light Transmission)	80 - 93 %
Dielectric Strength	15 - 22 kV/mm	Radiation Resistance	
Dissipation Factor	200 - 2000 10^{-4}	Gamma Radiation Resistance	Good
Volume Resistivity	14 - 16 10^{15} Ohm.cm	UV Light Resistance	
Polymethyl methacrylate	Physical Properties	Service Temperature	
Density	1.17 – 1.2 g/cm ³	HDT @0.46 MPa (67 psi)	80 - 110 °C
Glass Transition Temperature	90 - 110 °C	HDT @1.8 MPa (264 psi)	70 - 100 °C
Polymethyl methacrylate	Mechanical Properties	Max Continuous Service Temperature	70 - 90 °C
Elongation at Break	2 - 10 %	Others	
Elongation at Yield	2 - 10 %	Sterilization Resistance (Repeated)	Poor
Flexibility (Flexural Modulus)	2.5 – 3.5 GPa	Thermal Insulation (Thermal Conductivity)	0.15 - 0.25 W/m.K
Hardness Rockwell M	70 - 105		
Hardness Shore D	90 - 99		
Stiffness (Flexural Modulus)	2.5 – 3.5 GPa		
Strength at Break (Tensile)	38 - 70 MPa		
Strength at Break (Tensile)	38 - 70 MPa		
Toughness (Notched Izod Impact at Room Temperature)	10 - 25 J/m		
Young Modulus	2.5 – 3.5 GPa		

Table 2 Polymethyl methacrylate Chemical Properties [12].

Property	Value	Property	Value
Acetone @ 100%, 20°C	Non Satisfactory	Butylacetate @ 100%, 60°C	Non Satisfactory
Ammonium hydroxide @ 30%, 20°C	Satisfying	Chlorinated solvents @ 20°C	Non Satisfactory
Ammonium hydroxide @ diluted, 20°C		Diocetylphthalate @ 100%, 20°C	Limited
Aromatic hydrocarbons @ 20°C	Non Satisfactory	Ethanol @ 96%, 20°C	Limited
Aromatic hydrocarbons @ hot conditions	Non Satisfactory	Ethyleneglycol (Ethane diol) @ 100%, 20°C	Satisfying
Benzene @ 100%, 20°C	Non Satisfactory	Chloroform @ 20°C	Non Satisfactory
Butylacetate @ 100%, 20°C	Non Satisfactory	Diocetylphthalate @ 100%, 100°C	Non Satisfactory
Toluene @ 20°C	Non Satisfactory	Ethyleneglycol (Ethane diol) @ 100%, 100°C	Non Satisfactory
Toluene @ 60°C	Non Satisfactory	Methanol @ 100%, 20°C	Non Satisfactory
Xylene @ 20°C	Non Satisfactory	Methylethyl ketone @ 100%, 20°C	Non Satisfactory
Glycerol @ 100%, 20°C	Satisfying	Mineral oil @ 20°C	Satisfying
Kerosene @ 20°C	Satisfying	Phenol @ 20°C	Non Satisfactory
Sodium hydroxide @ 10%, 20°C	Satisfying	Silicone oil @ 20°C	Limited
Sodium hypochlorite @ 20%, 20°C	Satisfying		
Strong acids @ concentrated, 20°C	Limited		

1.3 BIOCOMPATIBILITY OF PMMA

The single most important factor that distinguishes a biomaterial from any other material is its ability to exist in contact with tissues of the human body without causing an unacceptable degree of harm to that body. The manner in which the mutually acceptable co-existence of biomaterials and tissues is developed and sustained has been of interest to biomaterials scientists and users of medical devices for many years. It has become clear that there are very many different ways in which materials and tissues can interact such that this co-existence may be compromised, and the search for biomaterials that are able to provide for the best performance in devices has been based upon the acquisition of knowledge and understanding about these interactions. These are usually discussed in the broad context of the subject of biocompatibility.

Biocompatibility is a word that is used extensively within biomaterials science, but there still exists a great deal of uncertainty about what it actually means and about the mechanisms that are subsumed within the phenomena that collectively constitute biocompatibility. As biomaterials are being used in increasingly diverse and complex situations, with applications now involving tissue engineering, invasive sensors, drug delivery and gene transfection systems, the medically oriented nanotechnologies and biotechnology in general, as well as the longer established implantable medical devices, this uncertainty over the mechanisms of, and conditions for, biocompatibility is becoming a serious impediment to the development of these new techniques [13].

1.4 ITACONIC ACID AND THE USES OF POLYITACONATE

Itaconic acid is a naturally occurring compound, non-toxic, and readily biodegradable. It is soluble in water, ethanol, and acetone. The dicarboxylic acid is a white crystalline, scentless powder. The molecular weight is 130.10 g/mol with a density of 1.63 g/cm³. Since the 1960s, it is biotechnologically produced industrially by the fermentation of carbohydrates such as

glucose or molasses using fungi such as *Aspergillus itaconicus* or *Aspergillus terreus*. For *A. terreus* the itaconate pathway is mostly elucidated. The generally accepted route for itaconate is via glycolysis, tricarboxylic acid cycle, and a decarboxylation of cis-aconitate to itaconate via cis-aconitate-decarboxylase [14]. The smut fungus *Ustilago maydis* uses an alternative route. Cis-aconitate is converted to the thermodynamically favoured trans-aconitate via aconitat- Δ -isomerase (Adi1) [15], trans-Aconitate is further decarboxylated to itaconate by trans-aconitate-decarboxylase (Tad 1). Itaconic acid is also produced in cells of macrophage lineage and as such, it has in vitro activity against bacteria expressing the enzyme isocitrate lyase such as *Salmonella enterica* and *Mycobacterium tuberculosis* [16]. However, cells of macrophage lineage have to "pay the price" for making itaconate, and they lose the ability to perform mitochondrial substrate-level phosphorylation. The generally accepted route for itaconate is via glycolysis, tricarboxylic acid cycle, and a decarboxylation of *cis*-aconitate to itaconate via *cis*-aconitate-decarboxylase.

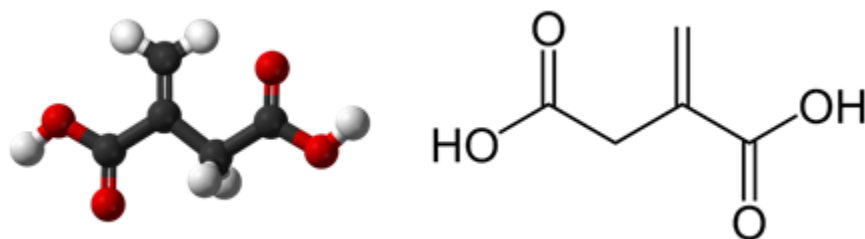


Figure 3 Structural formula representation of itaconic acid.

Itaconic acid is a fully sustainable industrial building block. It is primarily used as a co-monomer in the production of acrylonitrile-butadiene-styrene and acrylate latexes with applications in the paper and architectural coating industry.

1.5 INTRODUCING ITACONATE INTO PMMA IN ORDER TO OBTAIN BETTER BIOCOMPATIBILITY

Biomedical materials are one of the most attractive application areas of PMMA, where this material is used to create denture bases [6], bone cement [7], inhalers [8], *etc.* Materials based on PMMA are often used as biomaterials due to their good biocompatibility, non-toxicity, stability of color and shape [17], the absence of taste, smell and irritation of the surrounding

tissue [18], good adhesion to teeth, insolubility in body fluids, the ease of handling and design, as well as good aesthetic properties [19]. In spite of these advantages of the material, dental prosthesis based on PMMA have several drawbacks. The most important of these drawbacks are toxicity of residual monomer [20-22], susceptibility to distortions as well as limitations in terms of mechanics [23, 24]. Because of these deficiencies, residual monomer may leak out by diffusion from prosthesis and irritate the surrounding tissue. This leakage creates cracks and other structural damages to the dental prosthesis that could lead to mechanical fracture of the prosthesis and create an environment suitable for the development of different types of bacteria, moulds and fungi.

Biocompatibility of a material with a tissue means the compatibility with living tissue or a living system by not being toxic, injurious, or physiologically reactive and not causing immunological rejection in dentistry some special conditions are tested using materials foreign to the body in order to reestablish functionality. Biomaterials, generally, include polymers, metals, ceramics and composites. Some applications include materials that are in contact with the body and in those applications, the toxicity of the material is important. PMMA has a broad use as a material in dental applications, especially for the prophetic parts that are in contact with the mouth. Polymerization of PMMA is done using the catalyst and initiator and the quantity of the residual monomer determines the toxicity of the material. It was proven that the residual monomer in the polymer can be diminished using the addition of small quantity of methyl-itaconate. This addition reduces the residual monomer but also influences the material mechanical characteristics.

In order to overcome the drawbacks and the limitations of PMMA denture base materials, the possibility of modifying a commercially PMMA-based formulation using itaconic acid derivatives was investigated. Itaconic acid is structurally very similar to methacrylic acid, except that of the α -carbon atom a carboxyl group is attached instead of the H atom. Despite the slightly higher market price compared to methacrylic acid, itaconic acid and itaconates are more acceptable in terms of ecology and sustainable development [23, 25]. The reason for this lies in the fact that the itaconic acid is obtained from plants (mostly by enzymatic

transformations of molasses [6]), while methacrylic acid is derived from petrochemical sources. As a dibasic acid, itaconic acid provides more options when making its esters compared to methacrylic acid. Due to the many similarities of itaconates with the corresponding methacrylates and the mentioned advantages, itaconates represent an interesting alternative to methacrylates in the synthesis of a variety of materials.

In dentistry, itaconic acid and its esters are known. They have been widely used in the production of glass ionomer cements [26-28]. Itaconic acid and its derivatives are used as components in many systems for controlled drug release [29, 30]. It is important to note that itaconates have been extensively used in varying medical applications because of their very low toxicity [31]. Furthermore, itaconic acid and its derivatives are increasingly used in the preparation of paints and coatings [32, 33], composite resins [34, 35], contact lenses [36], and products for personal care [37].

Addition of itaconate derivatives to PMMA can decrease the content of residual monomer in the obtained product. Itaconates and methacrylates have similar structure and they can produce copolymers of ethyl methacrylate and dialkyl itaconates [21]. Fernandez-Garcia and Madruga [24] examined the effect of copolymer composition on the glass transition temperature and came to the conclusion that the glass transition temperature of the copolymers decreased with increasing amount of itaconate, as well as with the increasing alkyl chain length of the ester group. Investigation of the thermal stability of the copolymers of the methyl methacrylate and dialkyl itaconates showed that the relative thermal stability, increased with an increasing proportion of methyl methacrylate in the copolymer, following a similar trend as the change of glass transition temperature [23].

It was shown that the addition of itaconate led to a reduction in the water uptake and greatly reduced the residual methyl methacrylate content [38]. In this way, the applicative properties and biocompatibility of PMMA denture base materials for the production of dental prostheses were greatly improved.

It was found that the addition of diethyl itaconate to the PMMA significantly reduced the amount of residual methyl methacrylate, which made these materials less toxic. It was shown that increasing the DTHFI content resulted in materials with decreased glass transition temperatures, as well as with decreased storage modulus, ultimate tensile strength and impact fracture resistance; however the mechanical properties were in the rang prescribed by ADA standards, and the materials could be used in practice. The deterioration in mechanical properties was therefore worthwhile in order to gain lower the toxicity of the leached monomer [39].

2 COMPOSITE MATERIALS

A composite material is made by combining two or more materials – often ones that have very different properties but the overall properties could be designed and adjusted. The two materials work together to give the composite unique properties. It is always possible to distinguish the presence of the two materials that are making the composite material as they do not dissolve into each other. A composite material can be defined as a material system composed of two or more macro constituents that differ in shape and chemical composition and which are insoluble in each other. The history of composite materials dates back to early 20th century. In 1940, fiberglass was first used to reinforce epoxy.

In nature, composites could be found in as well as inside. Wood is a composite composed of long cellulose fibers (a naturally occurring polymer) held together by a much weaker substance called lignin. Cellulose is also found in cotton, but without the lignin to bind it together, it is much weaker. The two relatively weak substances – lignin and cellulose – together form a much stronger one.

The bones are also a composite, made from a hard but brittle material called hydroxyapatite (which is mainly calcium phosphate) and a soft and flexible material called collagen. On its own, collagen would not be much use in the skeleton but it can combine with hydroxyapatite to give bone the properties that are needed to support the body.

One early example of a composite material is mud bricks. Mud can be dried out into a brick shape to give a building material. It has good compressive strength but it breaks quite easily when loaded in tension. Straw seems very strong if you try to stretch it, but you can crumple it up easily. By mixing mud and straw together, it is possible to make bricks that are resistant to both squeezing and tearing and make excellent building blocks.

Concrete is a mix of aggregate, cement and sand. It has good compressive strength (it resists squashing). In more times that, are recent it has been found that adding metal rods or wires

to the concrete can increase its tensile strength? Concrete containing such rods or wires is called reinforced concrete.

Most composites are made of just two materials. One is the matrix or binder. It surrounds and binds together fibers or fragments of the other material, which is called the reinforcement. The binding of reinforcement to the matrix is of key importance for the composite strength and for the possibility to obtain the best possible properties of the composite. If this bond is too loose, the reinforcement cannot bare the load that the matrix is transferred and the overall composite has poor properties.

The biggest advantage of modern composite materials is that they are light as well as strong. By choosing an appropriate combination of matrix and reinforcement material, a new material can be made that exactly meets the requirements of a particular application. Composites also provide design flexibility because many of them can be molded into complex shapes. The downside is often the cost. Although the resulting product is more efficient, the raw materials are often expensive [40].

2.1 CLASSIFICATION OF COMPOSITE MATERIALS

Composites are defined as multiphase materials having significant proportions of each phase. The matrix is a continuous phase having the purpose to transfer stress to other phases, to protect phases from the environment. The matrix can be made of metal, ceramic or polymer, so the metal matrix composites MMC, ceramic matrix CMC and polymer matrix composites can be defined.

Dispersed phase, the phase that is supposed to carry the load can be in different forms, but depending on the matrix the purpose is in MMC to increase the strength and modulus of a material, in CMC the purpose is to increase ductility and in PMC the purpose is to increase the modulus, strength and to keep resisting. The form of the dispersed phase can be particles, fiber or the fibers can be made so to produce the textile structure to enable structural use of a composite. Figure 5 shows the schematic representation of the composite materials

classification based on the form of the reinforcement. The ways of reinforcement arrangements in polymer matrix are shown in Figure 6.

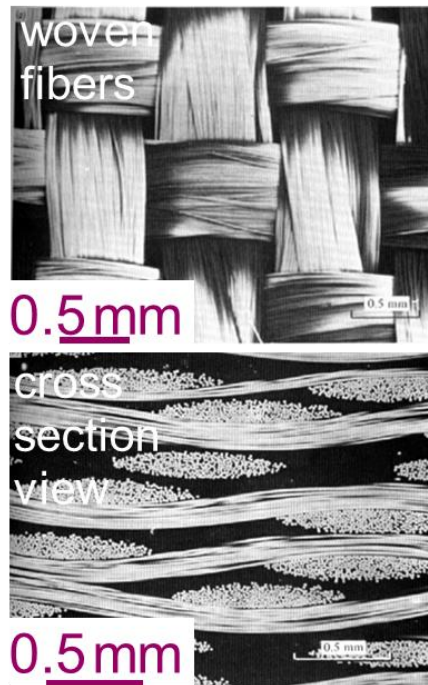


Figure 4 The phases present in a composite material, the fibers acting as a reinforcement are bound with a matrix material. The reinforcement can be distinguished from the matrix on a millimeter scale [41].

Dispersed phase, the phase that is supposed to carry the load can be in different forms, but depending on the matrix the purpose is in MMC to increase the strength and modulus of a material, in CMC the purpose is to increase ductility and in PMC the purpose is to increase the modulus, strength and to keep resisting. The form of the dispersed phase can be particles, fiber or the fibers can be made so to produce the textile structure to enable structural use of a composite. Figure 7 shows the schematic representation of the composite materials

classification based on the form of the reinforcement. The ways of reinforcement arrangements in polymer matrix are shown in Figure 6.

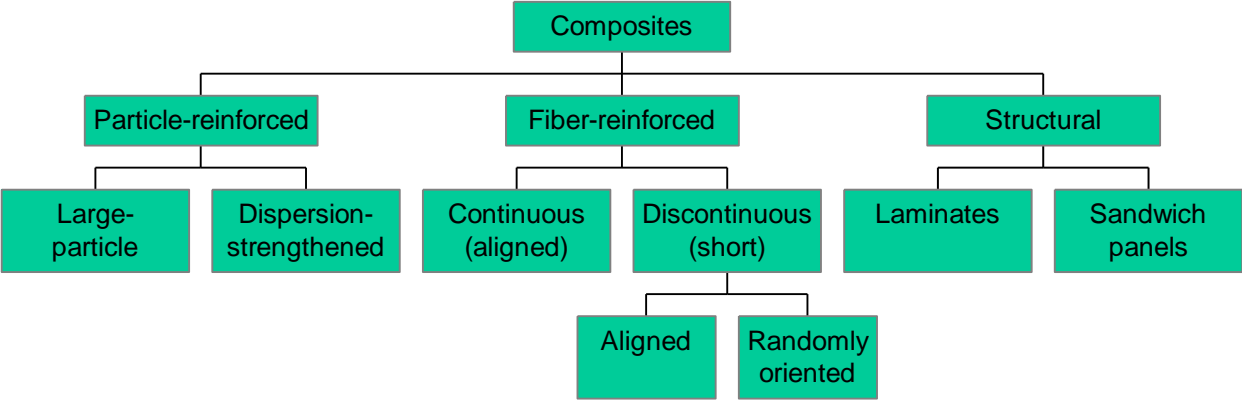


Figure 5 Schematic representation of composite materials classification [40].

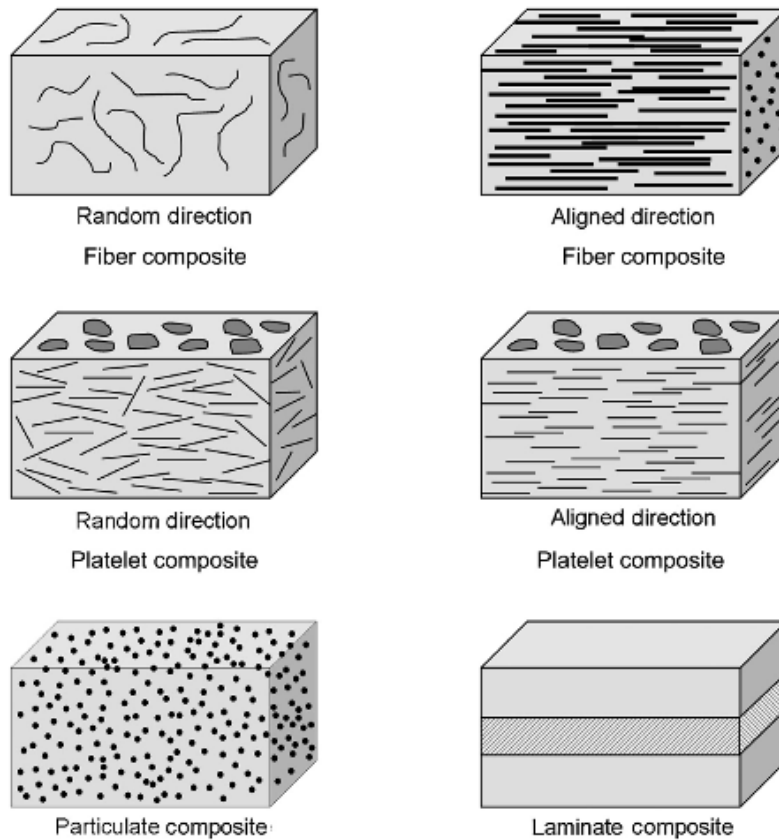


Figure 6 Ways of reinforcement arrangements in polymer matrix [42].

2.2 PARTICLE-REINFORCED COMPOSITES

Particles reinforce composites are the most widely used and among the cheapest composites. The size of the particles used as reinforcement determines the type of a composite, so large large-particle composites, act of restraining the movement of the matrix, if well bonded; and dispersion - strengthened composites, contain 10 - 100 nm particles and have a very large interphase area and exhibit more intense interaction between the particles and the matrix. The matrix bears the major portion of the applied load and the small particles hinder dislocation motion, limiting plastic deformation in MMC or in polymer matrix composites the particles take a significant part of the load as they are intensely connected to the matrix. The interphase

in those composites is of the uttermost importance for their mechanical and physical properties.

The reinforcement of polymer materials using nanoparticles is the important subject of research in recent years.

2.2.1.1 Large-Particle Composites

Properties are a combination of those of the components. The rule of mixtures predicts that an upper limit of the elastic modulus of the composite is given in terms of the elastic moduli of the matrix (E_m) and the particulate (E_p) phases by:

$$E_c = E_m V_m + E_p V_p$$

where V_m and V_p are the volume fraction of the two phases. A lower bound is given by:

$$E_c = \frac{E_m E_p}{(E_p V_m + E_m V_p)}$$

3 NANOSIZED REINFORCEMENT PARTICLES IN POLYMER MATRIX COMPOSITES

Reinforced rubber is obtained by strengthening with 20-50 nm carbon-black particles. Used in auto tires. This is one of the oldest examples of the use of sub micrometer sized particles in order to reinforce the matrix. The chemical bonding between the matrix and the reinforcement is of key importance to explain the behavior of such a composite. In recent years, the research in composite materials is based on this sort of materials. In this chapter, the intention is to present the recent research in alumina nano particles reinforced PMMA composites.

3.1 ALUMINA NANO PARTICLES

Alumina is the ceramic material having extraordinary chemical properties, used in composites for many years as a reinforcement, in analytical chemistry as adsorbent, as a catalyst in many chemical reactions as well as a material for high temperature applications. The stability and the high elastic modulus of corundum made one of the most used materials in high temperature applications. In composite materials, different structures of alumina that can be obtained in heat treatment are of special interest. The heat treatment can produce different structural materials that can be used in different applications.

Alumina (Al_2O_3) or aluminum oxide exists in nature as the mineral corundum (Al_2O_3); diaspore ($\text{Al}_2\text{O}_3 \cdot \text{H}_2\text{O}$); gibbsite ($\text{Al}_2\text{O}_3 \cdot 3\text{H}_2\text{O}$); and most commonly as bauxite, which is an impure form of gibbsite [43]. Alumina exists in numerous crystalline structures, such as χ -, η -, δ -, κ -, θ -, γ -, ρ - Al_2O_3 besides the thermodynamically stable α - Al_2O_3 (corundum). Metastable phases, usually called “transition alumina” phases may be irretrievably translated to α - Al_2O_3 by appropriate thermal or hydroxylation treatments [44, 45]. Figure 7 displays the pathways of transition Al_2O_3 during heat treatment. The crystal structure of alumina comprises hexagonal and octahedral sites [46].

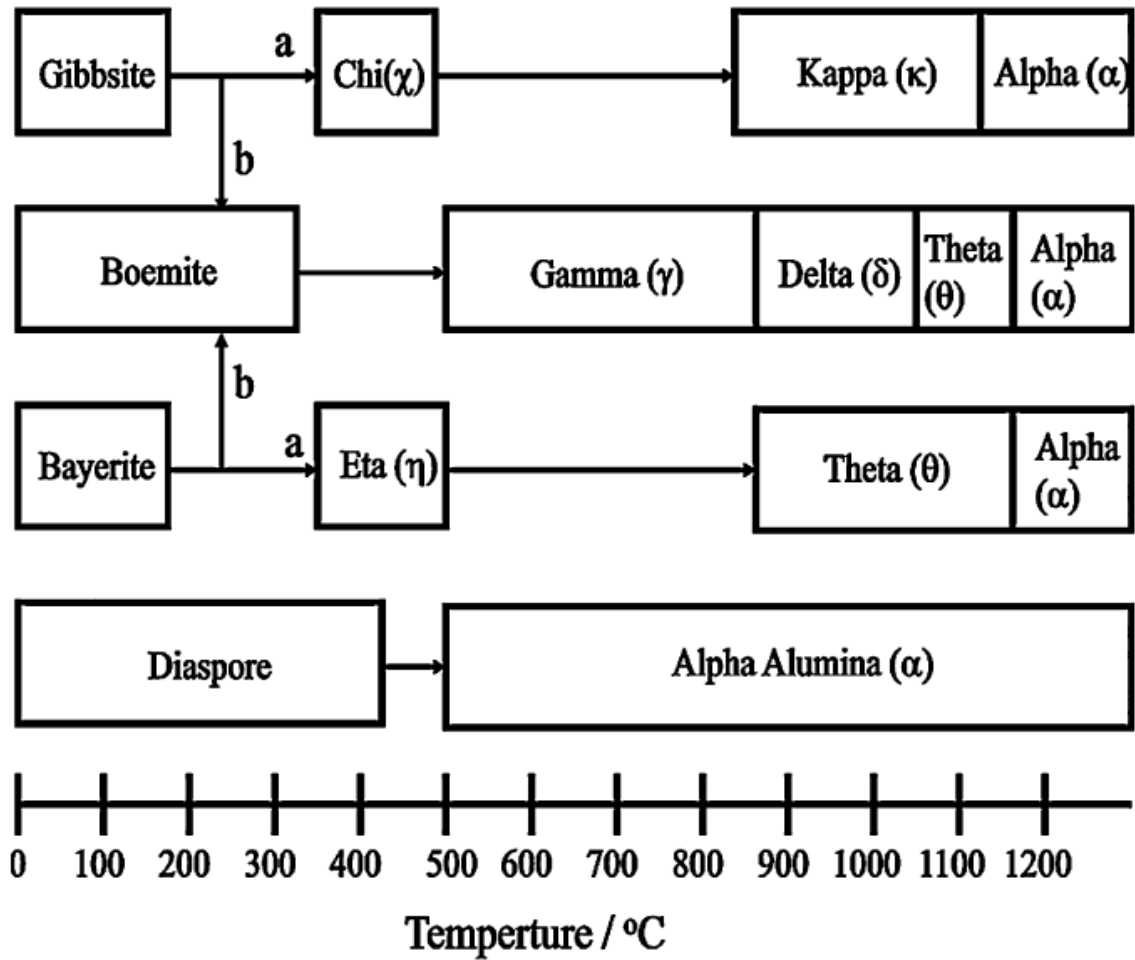


Figure 7 Structure transformation of alumina and aluminum hydroxides [47].

Various reports conclude that the average crystal-size of the Al_2O_3 powder increases with increasing calcination temperature. During the growth rate of particles increases more quickly than the nucleation rate and the agglomeration tendency of particles becomes stronger. Therefore, a low calcinations temperature is required to form particles with a small and narrow size distribution [48, 49].

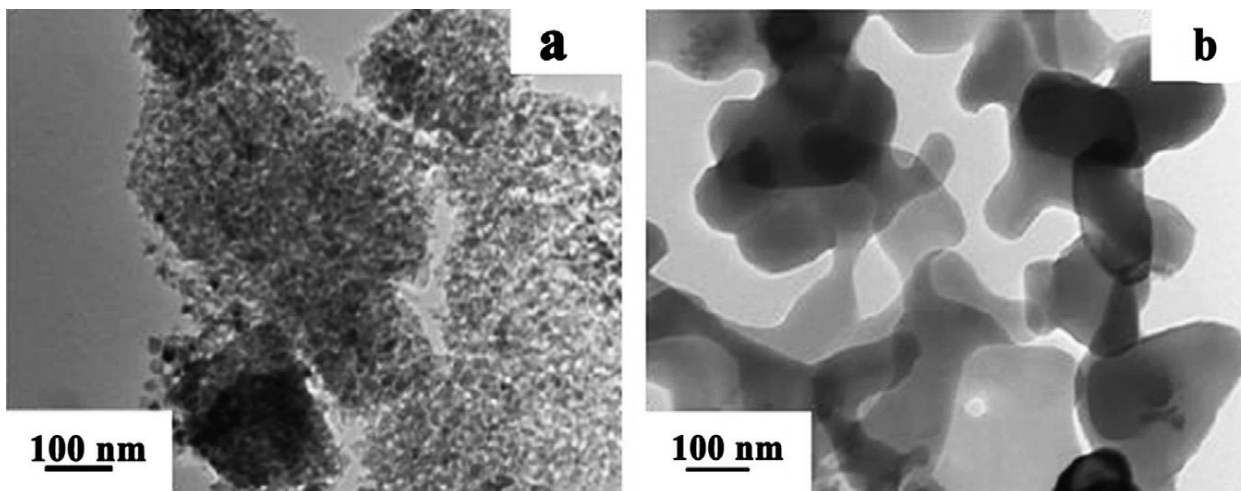


Figure 8 TEM micrographs of unseeded powders after calcination (a) 1000 °C and (b) 1200 °C [49].

There are several different methods of synthesis of Al₂O₃ nanoparticles: reverse micelle [50], sol–gel processing [51, 52], flame spray pyrolysis [53], precipitation [54], hydrothermal [55] and combustion method [56]. In metal oxides, the surface of a solid crystal is a truncated area of the crystal consisting of coordinately unsaturated site anions and cations. For this reason, when a metal oxide is exposed to the atmosphere, the outer layer becomes covered with the abundant component, such as water. This absorbed water can be present at the surface in the form of the terminal OH groups [57]. Among the different metal oxide nanoparticles, those made of alumina have a range of useful properties, including good thermal conductivity, high strength and stiffness, mechanical strength, inertness to most acids and alkalis, high adsorption capacity, wear resistance, oxidation, thermal stability and electrical insulation... In addition, it is inexpensive, nontoxic, and highly abrasive [58-60]. Many of the mechanical and physical properties associated with Al₂O₃ nanoparticles. These physicochemical properties propose Al₂O₃ nanoparticles with great potential to fit a specific application in the field of the pigments, porous ceramic membranes, catalysts or catalyst carriers, ultra-filtration membranes, electrical insulators, high voltage insulators, furnace liner tubes, ballistic armor, abrasion resistant tube and thermometer sensors [59, 60, 61].

3.2 ALUMINA NANOPARTICLES REINFORCED PMMA

Different alumina filler can have different impacts on mechanical properties of the resulting composite. Addition of different shaped alumina fillers was investigated using the nanoindentation technique measuring the hardness and modified modulus of the resulting materials. Three different fillers were used; spherical nanoparticles, alumina whiskers and electrospun nano fibers were used as fillers. It was observed that up to 5 wt. % of added product dramatically changes the mechanical properties of the composite [62]. Mean values for reduced elastic modulus and hardness measured using nanoindentation are presented in Figure 9. The addition of 1 wt. % of any of the used fillers did not improve the hardness values. The addition of 3 wt. % of the whiskers and electrospun alumina product resulted in improvements in the reduced elastic modulus and hardness, whereas the addition of the spherical nanoparticles did not improve significantly the hardness of the obtained composite. The improvement of elastic modulus for the addition of electrospun product was 134 % compared to the polymer without any additions. The addition of 5 wt. The % electrospun product did not improve the values of the reduced modulus. Furthermore, the hardness values significantly improved to 157.8 % in addition of 3 wt. % electrospun product, while the improvement of the hardness was 120.2 % for the sample containing 5 wt. % of electrospun product as seen in Figure 9.

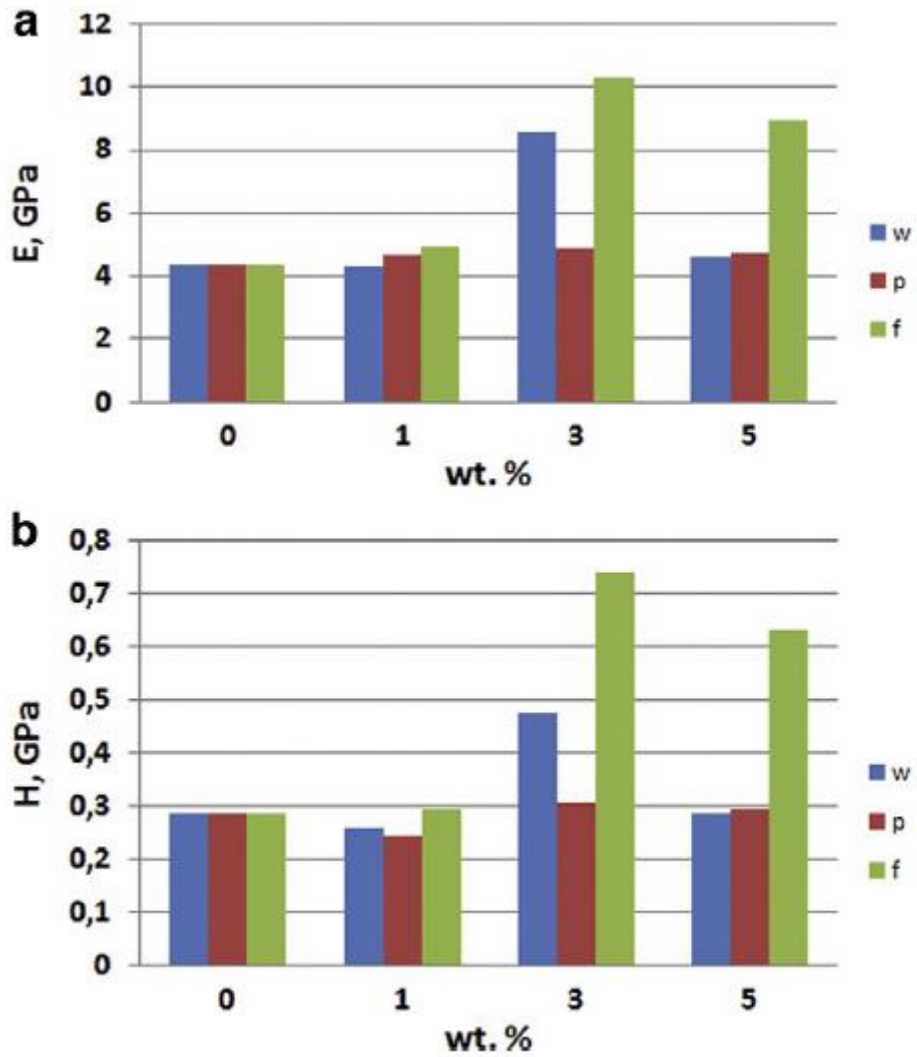


Figure 9 Mean values of reduced elastic modulus and hardness measured using the nanoindentation technique for specimens containing different fillers.

4 CHARACTERIZATION METHODS

4.1 PARTICLE SIZE AND MORPHOLOGY ANALYSIS

The distribution of the filler particles was determined using an optical microscope and the laser particle size analyzer (PSA) Mastersizer 2000. The laser particle size analyzer (PSA) Mastersizer 2000 was used to measure the particle size distribution, which covers the particle size range of 0.02–2000 μm .

Morphology and shape of the particles were observed using a Mira3 Tescan field emission scanning electron microscope (FE-SEM), operated at 20 kV. The samples were previously coated with a thin gold film. The particle size and the dispersion of synthesized fillers were obtained by image analysis using the Image Pro Plus 6.0 software. Images from FE-SEM was further used for measuring diameters and particles morphological parameters. Particle size distribution and particle shape characterization were determined from further analysis of those data. The morphologies of the composites with different alumina-based particles were examined using a field emission scanning electron microscope (FESEM), MIRA3 TESCAN, operated at 3 kV.

4.2 CRYSTAL STRUCTURE ANALYSIS

The X – ray powder diffraction was performed using a Bruker D8 Advance diffractometer in Bragg-Brentano transmission mode θ/θ with the primary germanium (Ge (111)) monochromator of Johannson type ($\text{CuK}\alpha_1$ radiation, $\lambda=1.54059 \text{ \AA}$). The diffraction data were collected by using a scintillation counter of NaI (TI) type and the scan-step method in the range of 2θ diffraction angle from $10\text{-}90^\circ$, with a step size of 0.05° and counting time of 6 s per step.

4.3 FT-IR STRUCTURE ANALYSIS

The structural analysis of synthesized and at different temperatures calcined powders was performed by single-beam Fourier-Transfer Infrared Spectroscopy (FTIR) using a Nicolet 6700 spectrometer (Thermo Scientific) in the attenuated total reflectance (ATR) mode using a single bounce 45 °F Golden Gate ATR accessory with a diamond crystal, and an electronically cooled DTGS detector. The spectra were the co-addition of 64 scans at 4 cm^{-1} spectral resolution, and were ATR corrected. The Nicolet 6700 FT-IR spectrometer was equipped with OMNIC software and recorded the spectra in the wavelength range from 2.5 to $20\text{ }\mu\text{m}$ (*i.e.*, 4000 cm^{-1} to 500 cm^{-1}).

4.4 MECHANICAL TESTING

Mechanical testing was accessed by several methods in order to obtain the relevant data for the material behavior in different situations. So microhardness was used to test the surface of the material, tensile testing and bending were also used to obtain corresponding modulus and finally the impact testing was used to obtain data about the toughness of the material.

4.4.1 Microhardness measurements

The micro hardness of the composite systems was characterized using micro Vickers hardness (HV) tester Leitz, Kleinharteprüfer DURIMETI using an original quadrangular pyramid diamond indenter with an angle of 136° [63]. In order to obtain reproducible HV value micro hardness of PMMA composites without particles and PMMA composites with different alumina-based particles was measured applying a load of 500 g for 25 s. For each sample, three indents were performed at room temperature according to ASTM E384-16 [64]. Image Pro Plus program was used to obtain the diagonal lengths from images obtained by the optical microscope, Carl Zeiss – Jena, NU2. The average results of diagonal were taken as the reported measurement for calculation of micro hardness using the following equation:

$VHN = 2 \cos \frac{22^\circ P}{d^2} = \frac{1.8544P}{d^2}$, where P (kgf) is the applied load and d (mm) is the length of the indentation diagonal [65].

Tensile testing was performed on the hydraulic machine, Instron Testing Machine (model number 6025) with the data acquisition system that monitored the deformation and force. The specimen for tension test had standard dimensions having the cross-section in the testing area of 2 mm x 5 mm and the length was 5 cm. The obtained data were used to measure the tensile properties of the composite. From every group, three specimens were taken for the measurement and the results were presented as the mean values of three different measurements.

4.4.2 Toughness measurements

The impact energy tests of the composites were performed on High-Speed Puncture Impact testing machine HYDROSHOT HITS-P10, Shimadzu, Japan. Total absorbed energy is calculated automatically corresponding to the load-time diagram, offering the energy values for the maximum load and puncture point. The puncture point was defined as the point where the force drops to zero value. The striker with a hemispherical head (diameter 12.7 mm) was loaded with the programmable impact velocity set at 1 m/s. Sampling time was 10 μ s and 12000 sampling points were acquired, some before and most during and after the impact for samples with PMMA and alumina based particles but sampling time was 500 μ m for PMMA/DMI/ Al_2O_3 composite materials. The striker was set to puncture all the considered samples. From every group, three specimens were taken for the measurement and the results were presented as the mean values of three different measurements.

In order to measure the resistance of presenting composite materials to the high speed impact the materials were tested to the resistance to the impact of controlled energy. The Impact energy tests were performed on High Speed Puncture Impact testing machine HYDROSHOT HITS-P10, Shimadzu, Japan, Figure 10. The composites reinforced with the commercial alumina nanoparticles and synthesized alumina submicron particles and the ones with ferrous

oxide doped alumina were tested. The obtained results gave the information about the behavior of the composite in the situation of impact induced by a sudden hit.



Figure 10 The specimen for high speed impact testing in the testing machine after the impact.

4.4.3 Residual monomer determination

The residual monomer from prepared composites was extracted with methanol in accordance to a procedure previously reported [21]. A Surveyor LC system (Thermo Fisher Scientific, Waltham, MA, USA) was used for the separation of the analyses on a reverse-phase Zorbax Eclipse[®]XDB-C18 column, 4.6 mm × 75 mm internal diameter and 3.5 μm particle size (Agilent Technologies, Santa Clara, CA, USA). In front of the separation column, a pre-column was installed; 4.6 mm × 12.5 mm internal diameter and 5 μm particle size (Agilent Technologies).

Bend or flexure testing is common in springs and brittle materials whose failure behaviors are linear such as concretes, stones, woods, plastics, glasses and ceramics. Other types of brittle materials such as powder metallurgy processed metals and materials are normally tested under a transverse flexure. Bend test is therefore suitable for evaluating the strength of brittle materials where interpretation of tensile test result of the same material is difficult due to breaking of specimens around the specimen gripping. The evaluation of the tensile result

is therefore not valid since the failed areas are not included in the specimen gauge length. Smooth rectangular specimens without notches are generally used to bend testing under Figure 11 illustrates three-point bending.

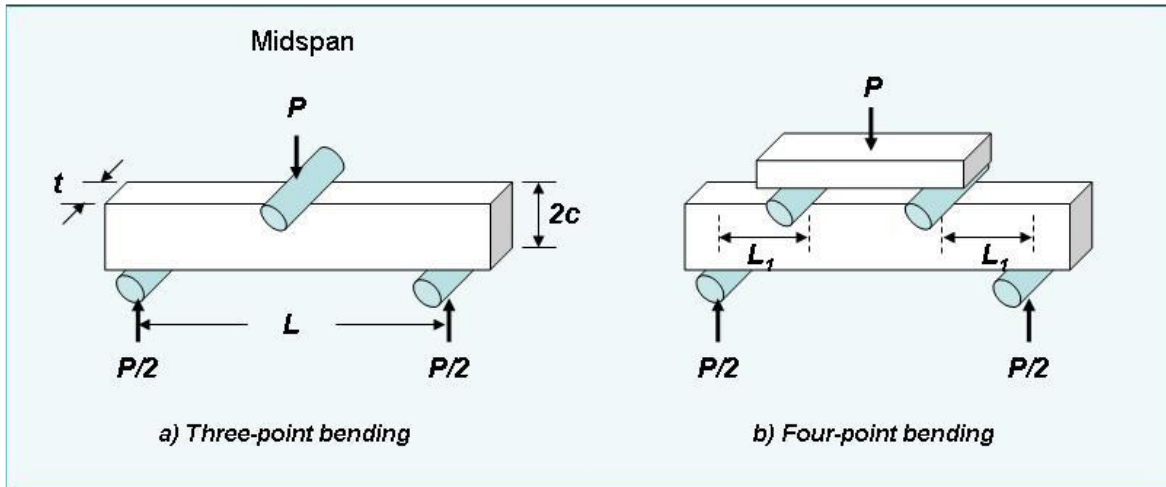


Figure 11 Bend testing of a rectangular bar under a) three-point bend and b) four-point bend arrangements.

Considering a three point bend test of an elastic material, when the load P is applied at the midspan of specimen in an x - y plane, stress distribution across the specimen width ($w = 2c$). The stress is essentially zero at the neutral axis N - N . Stresses in the y -axis in the positive direction represent tensile stresses whereas stresses in the negative direction represent compressive stresses. Within the elastic range, brittle materials show a linear relationship of load and deflection where yielding occurs on a thin layer of the specimen surface at the midspan.

This in turn leads to crack initiation, which finally proceeds to specimen failure. Ductile materials however provide load-deflection curves, which deviate from a linear relationship before failure takes place as opposed to those of brittle materials previously mentioned. Furthermore, it is also difficult to determine the beginning of yielding in this case. The stress distribution of a ductile material after yielding is given in Figure 11b). Therefore, it can be seen that bend testing is not suitable for ductile materials due to difficulties in determining

the yield point of the materials under bending and the obtained stress-strain curve in the elastic region may not be linear. The results obtained might not be validated. As a result, the bend test is therefore more appropriate for testing of brittle materials whose stress-strain curves show its linear elastic behavior just before the materials fail.

For brittle materials having a linear stress-strain relation, the fracture stress equals:

$$\sigma = \frac{Mc}{I} = \frac{3M}{2tc^2} \text{ where } I = \frac{2tc^3}{3}$$

where M is the bending moment

c - is half of the specimen width as shown in Figure 10a

t - is the thickness of the specimen as shown in Figure 10a.

I - is the moment of inertia of the cross-sectional area.

Under three-point bending in **Error! Reference source not found.** a) when the load P is applied at the midspan of a rectangular bar of a length L between the two rollers, the highest bending moment at the midspan is

$$M = \frac{PL}{4}$$

We then have

$$\sigma_{fb} = \frac{3LP_f}{8tc^2} = \frac{3LP_f}{2tw^2}$$

where

σ_{fb} is the calculated fracture stress

P_f is the fracture load obtained from the bending test

w is the width of the specimen of length = 2c

The fracture stress in bending is called the bend strength or flexure strength, which is equivalent to the modulus of rupture in bending. The bend strength is slightly different from the fracture stress obtained from the tensile test if failure takes place further away from yielding. However, brittle materials possess higher strength in compression than in tension.

The determination of the yield strength (σ_y) is carried out by replacing the load at yielding P_f . The yielding load is determined at the definite yield point or at certain % offset.

Hence, we now have the yield strength, it should be noted that the yield strength obtained from the bend test is not different from the yield strength achieved from the tensile test. This is because the relationship between the load and the deflection remains linear at yielding.

$$\sigma_0 = \frac{3LP_y}{2tw^2}$$

The flexural strain ε_f is calculated as

$$\varepsilon_f = \frac{6wv}{L^2}$$

Moreover, from the experimental result, we can also obtain the elastic modulus of the material according to the linear-elastic analysis. The deflection of the beam (v) from the can be expressed as

$$v = \frac{PL^3}{48EI}$$

where the elastic modulus (E_B) can be calculated from the slope of the load-deflection curve $\frac{dv}{dP}$ in the linear region as follows

$$E_B = \frac{L^3}{48I} \left(\frac{dP}{dv} \right) = \frac{L^3}{32tc^3} \left(\frac{dP}{dv} \right) = \frac{L^3 m}{4tw^3}$$

Where m is the slope of the tangent to the straight-line portion of the load-deflection beam. The elastic moduli achieved from the bend test are generally close to the elastic moduli obtained from tension and compression using the same material. However, there are several factors that might affect the elastic moduli, which are 1) elastic and plastic deformation at the rollers at the supports or the loading points might not be sufficiently small in comparison

to the beam deflection. 2) If a short specimen is bend tested, deformation due to shear stress may take place, which are not ideal for the calculation according to the beam theory. 3) Materials might have different elastic moduli under bending, tension and compressive. Therefore, the elastic moduli in bending should be identified with any avoid confusions for the interpretation of the mechanical behavior of the material.

5 EXPERIMENTAL PART

The aim of the experimental part of this thesis was to synthesize a convenient composite material responding to several demands. The experimental procedure was selected so to obtain different combinations of a PMMA as a matrix and to synthesize different reinforcing particles so as to obtain the composite having improved mechanical properties. The other point that was addressed in this work was the use of a copolymer of PMMA modified using the ethyl itaconate and so diminish the quantity of the monomer in the resulting material. It was proved that this way was the good one to improve the biocompatibility of a composite. The addition of different reinforcement not only improved the mechanical properties, but also further diminished the quantity of a residual monomer. All the composites synthesized in this work were conform to the demands of the industrial applications that are set for the use in dentistry.

The aim of this part of the study was to control the mechanical properties of the composite material using the industrial PMMA material and synthesized alumina particles and in order to influence the crystal structure alumina particles doped with the ferrous oxide.

5.1.1 Materials and sample preparation

The composite consists of a PMMA (the commercial Biocryl, Galenika AD, Serbia) powder contains the addition of catalyst and the liquid component MMA (Galenika AD, Serbia) with the initiator. Aluminum hydroxide chloride (Locron L; $\text{Al}_2(\text{OH})_5\text{Cl} \cdot 2,5 \text{H}_2\text{O}$) was purchased in the crystallized state from the Clariant company.

Two types of alumina-based particles were synthesized using the sol-gel technique. The starting components were $\text{Al}_2\text{Cl}(\text{OH})_5 \cdot 2,5 \text{H}_2\text{O}$ and demineralized water. These components were mixed on the magnetic stirrer until the aluminum hydroxychloride was completely dissolved and then put into a petri dish and allowed to dry. The gel was milled in laboratory

mortar. The powder was calcinated at three different temperatures: 700, 800 and 900 °C, for 2h, to obtain different crystalline structures. The same procedure was repeated for the production of aluminum oxide particles doped with Fe₂O₃. To the sol composed of Al₂Cl(OH)₅·2.5 H₂O and demineralized water, 1.5 wt.% FeCl₃·6H₂O (Sigma-Aldrich) was added and it was left to gelify. These particles were also thermally treated at 700 °C, 800 °C and 900 °C for 2 h. Obtained particles were of submicron size. Alumina nano-particles (Sigma-Aldrich) were used as received from the producer (spherical alumina nanoparticles < 50 nm).

5.1.2 Specimen preparation

The first type of specimens were made of the pure PMMA in order to compare the properties of the matrix to the properties of obtained composites. Composites were prepared using the PMMA matrix with the addition of 3 wt. % of alumina-based particles. The particles were dispersed in a monomer-liquid component with an ultrasonic bath. Ultra-sonication lasted for 1 hour in order to avoid agglomeration and to obtain a good dispersion. The powder component (PMMA) was added to the liquid and the mixture turned into a paste that was then put into a mold made of aluminum alloy. The mold was closed and then heat-treated at 70 °C for 1 hour to polymerize. Completion of the polymerization was done at 100 °C during 30 min to diminish the residual monomer content.

The second type of specimens were made of the commercial Biocryl as the source of PMMA and dimethyl-itaconate as the source for itaconate were used. The preparation of PMMA is based on a two component system, the powder contains the polymerized PMMA with the addition of catalyst and the liquid component with the initiator and the monomer. The Itaconate was added to a monomer together with selected particles and this was treated using the ultrasonic bath. Ultra sonication was done during 30 min in order to avoid agglomeration and to obtain a good dispersion. The powder component was added to the liquid and in approximately 5 min the mixture turned into a paste that was then put into a mold made of aluminum alloy. The mold was closed and then heat treated at 70 °C to obtain polymerization without the boiling of the monomer present and finalization of the polymerization was done

at 100 °C during 1h. The obtained specimen was used in a tensile test, three point bending test and high-speed impact-testing machine. For all matrix materials, the copolymer of PMMA and diethyl itaconate was used. The specimens were prepared using 1, 3 and 5 wt. % spherical nano-alumina particles and the same amount of ferrous doped alumina particles. Mold for the preparation of samples and samples made for tensile testing, 3 point bending testing and high speed impact testing are shown in Figure 12.



Figure 12 a) The mold for sample preparation showing the forms for preparation of the sample for tensile testing, for 3 point bending testing and for high speed impact testing, b) The specimens for tensile testing and 3 point bending testing just after being prepared.

6 RESULTS AND DISCUSSION

The results of this research are presented in several parts so as to show the characterization of obtained reinforcement particles, to present and discuss the results of mechanical testing of obtained composites and to show the quantity of a residual monomer in the synthesized composite.

6.1 PARTICLE SIZE DISTRIBUTION OF SYNTHESIZED ALUMINA PARTICLES

Particle size distribution indicated narrow distribution of synthesized alumina particles in the interval between 0.3 and 1.3 μm , with a maximum peak at 0.48 μm (Figure 13). Measurements of particle size distribution according to the volume fraction showed higher values of diameters ($\sim 20 \mu\text{m}$) suggesting the complex shape of synthesized alumina particles. In order to investigate this presumption particles were analyzed by FE-SEM.

The lower particle size of $\text{Al}_2\text{O}_3 \text{ Fe}$ than $\text{Al}_2\text{O}_3 \text{ m}$ may lead to the presumption that $\text{Al}_2\text{O}_3 \text{ Fe}$ could provide better load transfer and stabilization prolonging the moment of composite failure.

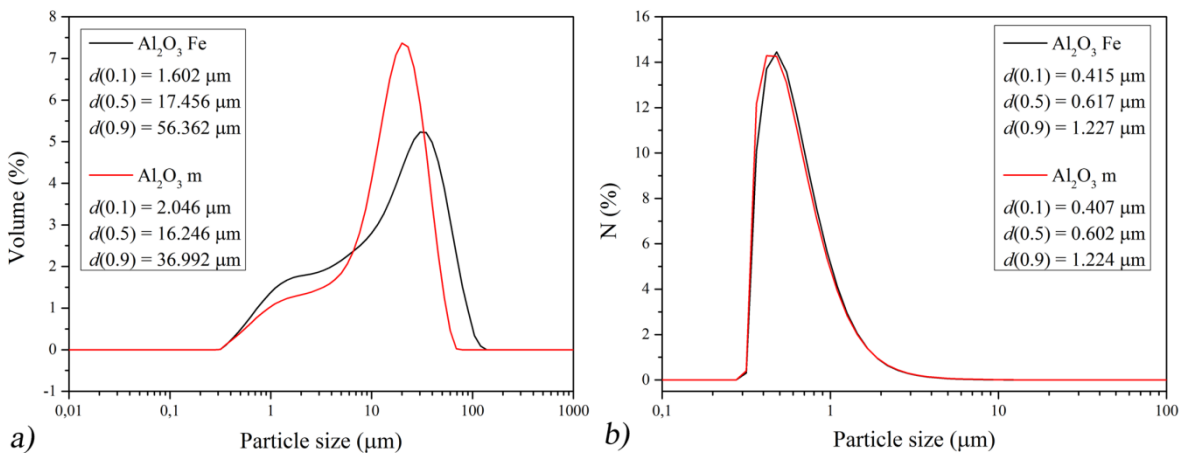


Figure 13 Particle size distribution of synthesized alumina particles (Al_2O_3 Fe and Al_2O_3 m) obtained from Mastersizer [66].

6.2 PARTICLE MORPHOLOGY OBTAINED FROM FE-SEM ANALYSIS

Morphology and shape of the particles were observed using a field emission scanning electron microscope (FE-SEM). Figure 14 showed increased specific surface area of synthesized alumina particles that enable better interface contact with the matrix and thus may improve the adhesion between the filler and the matrix. The presence of higher amount of single nanoparticles on the surface of micro-sized particles are the reason for the difference between the particle size distribution according to the number and volume. The particle size and the dispersion of synthesized fillers were obtained by image analysis using the Image Pro Plus 6.0 software. Analyzing images from the FE-SEM and processing by Image Pro Plus software, the size distribution of $\text{Al}_2\text{O}_3\text{m}/\text{Al}_2\text{O}_3\text{Fe}$ particles showed mostly submicron range of diameters achieved by sol-gel technique. Measured diameters of the particles (Table 3) suggest the presence of a higher amount of single nano/submicron particles on the surface of Al_2O_3 m then on the surface of Al_2O_3 Fe. The obtained values for particle size were in accordance with the range of particle size distribution from Mastersizer (Figure 15) suggesting that the most of agglomerates dissipated on single submicron particles. FE-SEM showed the roughness of calcinated particle surface compared to the smooth one seen since α - Al_2O_3 [67]. Such microstructure of Al_2O_3 Fe and Al_2O_3 m particles were in agreement with the XRD analysis that proved mostly transition alumina composition that is more characteristic with a higher specific surface area than α - Al_2O_3 .

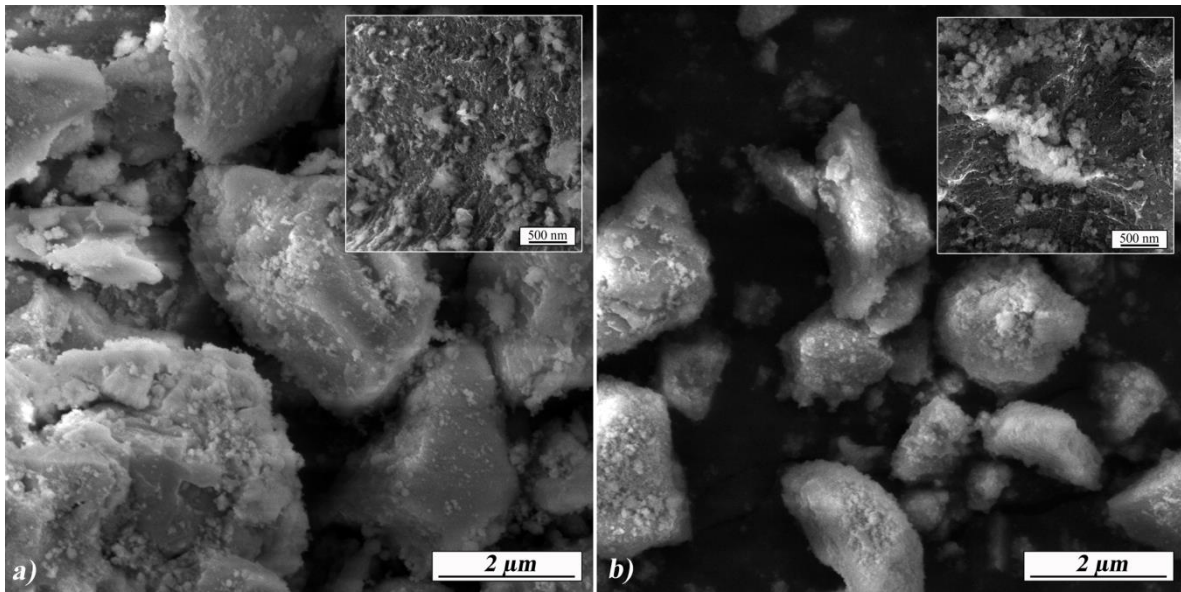


Figure 14 FE-SEM images of surface morphology of synthesized alumina particles: a) Al_2O_3 m, b) Al_2O_3 Fe with a magnified part to obtain an insight into the surface roughness [66].

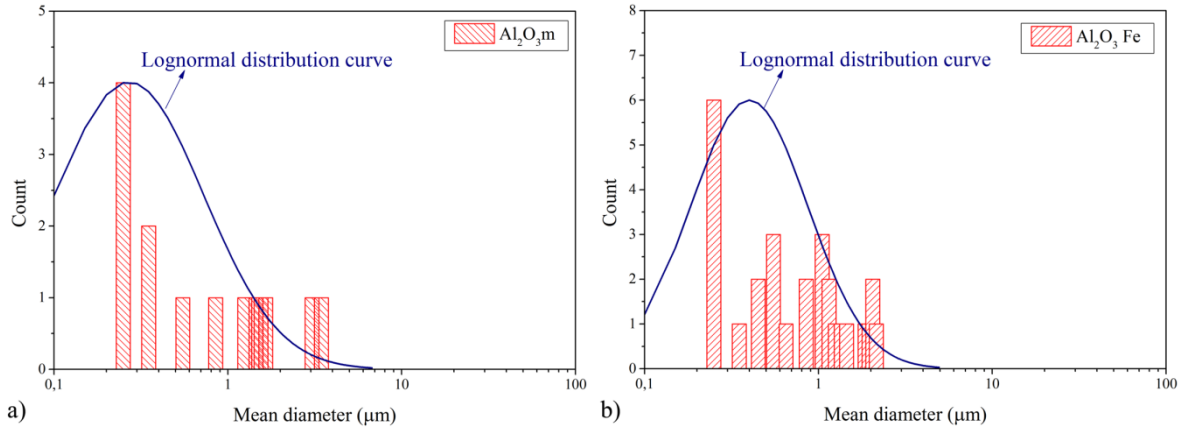


Figure 15 Mean diameter distribution obtained from image analysis for synthesized particles: a) Al_2O_3 m, b) Al_2O_3 Fe [66].

Table 3 Statistical data of mean values of particle size obtained by image analysis [66].

Particle	Area, μm^2	Max diameter, μm	Min diameter, μm	Mean diameter, μm	Roundness	Fractal dimension
Al ₂ O ₃ m	0.27 ± 1.20	0.33 ± 0.76	0.17 ± 0.18	0.24 ± 0.38	2.17 ± 2.25	1.10 ± 0.05
Al ₂ O ₃ Fe	0.35 ± 0.86	0.51 ± 0.78	0.25 ± 0.40	0.35 ± 0.54	2.09 ± 0.94	1.10 ± 0.04

The results presented are showing that the particles after a calcination procedure are heavily agglomerated and that the procedure in composite preparation should incorporate the method to deagglomerate those particles and obtain a homogeneous composite material. When the particles were analyzed using the Master Sizer machine it was obvious that the particles could be deagglomerated and that the submicron particles were obtained. Those were the promising results for the synthesis of the composite.

6.3 MICROSTRUCTURE OF THE PARTICLES AND PMMA COMPOSITES

The morphology and the size distribution of alumina-based particles with marginal values of crystal phases (Al₂O₃ 700 °C and Al₂O₃ Fe 900 °C) were examined using scanning electron microscopy and image analysis. In Figure 16a, the micrograph of the particles calcinated at 700 °C is given and in Figure 16b the micrograph of the composite having 3 wt. % of the synthesized alumina particles is presented. These images were used to measure the diameters of the synthesized alumina particles.

The results of diameter measurements presented in Figure 16c and Figure 16d show that the mean diameter of synthesized alumina particles indicate that agglomerate size decreased from 2.73 μm to 0.33 μm (87.9%) in the composite containing 3 wt. % of synthesized alumina particles. The appreciable reduction in the sizes of the visible agglomerates of the synthesized alumina particle indicates that the agglomerates dimensions were reduced and that synthesized alumina particles were well distributed in the polymer, bringing improvements in the mechanical properties.

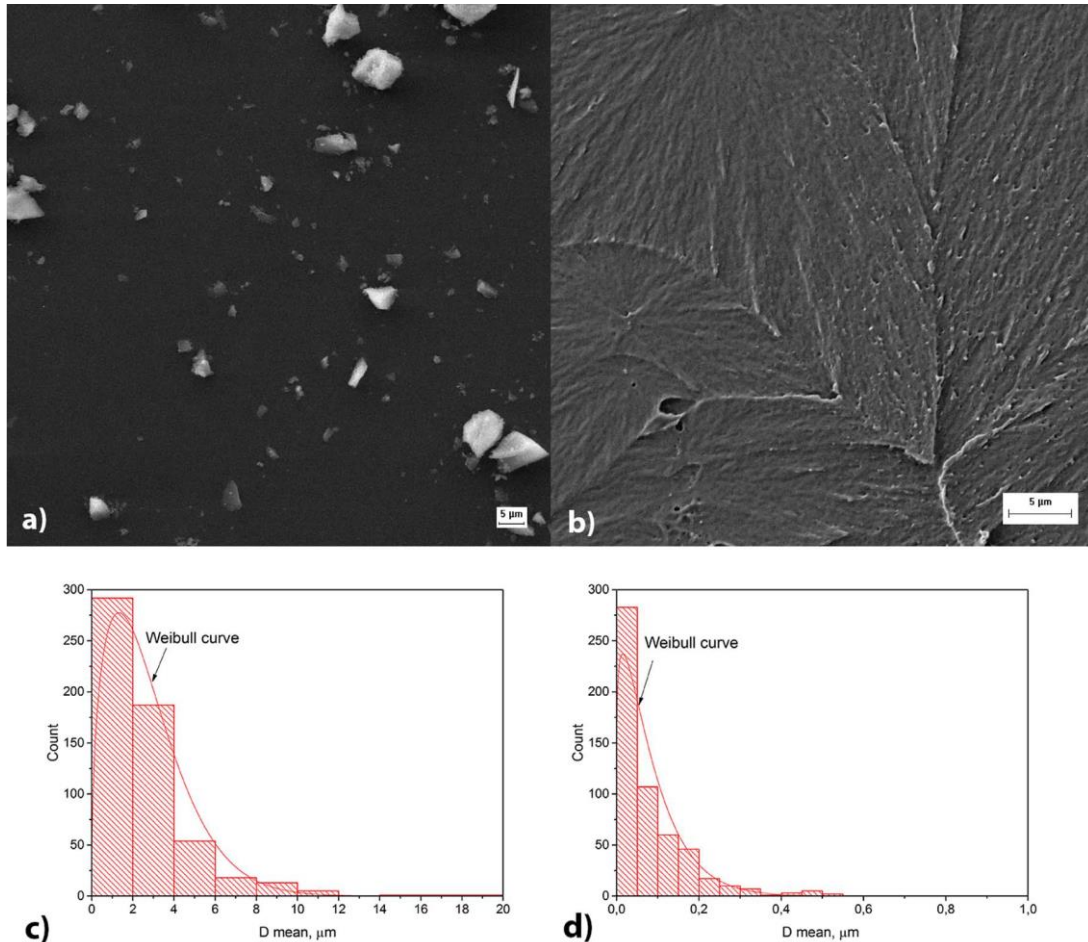


Figure 16 The FESEM micrographs of: *a) agglomerates of synthesized alumina particles, b) composite having PMMA matrix and 3 wt. % of synthesized alumina particles at 700 °C, c) distribution of the diameter of synthesized alumina particles sintered at 700 °C, d) distribution of the diameter of synthesized alumina particles dispersed in composites [68].*

In Figure 17a the micrograph of the fractured surface of ferrous oxide doped alumina particles sintered at 900 °C and in Figure 17b the micrograph of the composite having 3 wt. % of the ferrous oxide doped alumina particles is presented. Those samples are selected as the composite prepared using the alumina ferrous-doped particles calcinated at 900 °C shows the best improvement of hardness, while the specimen prepared using the alumina particles calcinated at 700 °C exhibits the lowest improvement of hardness. The mean diameter of ferrous oxide doped alumina particles agglomerates decreased from 3.44 μm to 0.41 μm

(88.1%) in the composite containing 3 wt. % of ferrous oxide doped alumina particles, Figure 17c and Figure 17d. It can be noticed that the percentage reduction in particle size was almost identical for both particles suggesting that they exhibit the similar interactions with the polymer matrix. During the conversion to α phase, the particle size increases since the crystal defects are gradually reduced, and they completely disappear with the accomplishing the crystallization of α phase [64].

Table 4 *The results of pore volume and surface areas of the of alumina-based particles and ferrous oxide doped alumina particles [68].*

Alumina Particles	Pore volume, cm^3g^{-1}	Surface area, m^2g^{-1}	Median pore diameter, nm	Maximum pore diameter, nm	Cumulative pore volume, cm^3g^{-1}	Cumulative pore area, m^2g^{-1}
Al_2O_3 700 °C	0.1695	96.404	7.2466	5.5081	0.1679	102.44
Al_2O_3 +Fe 900 °C	0.2163	89.717	10.87	7.4741	0.2339	101.18

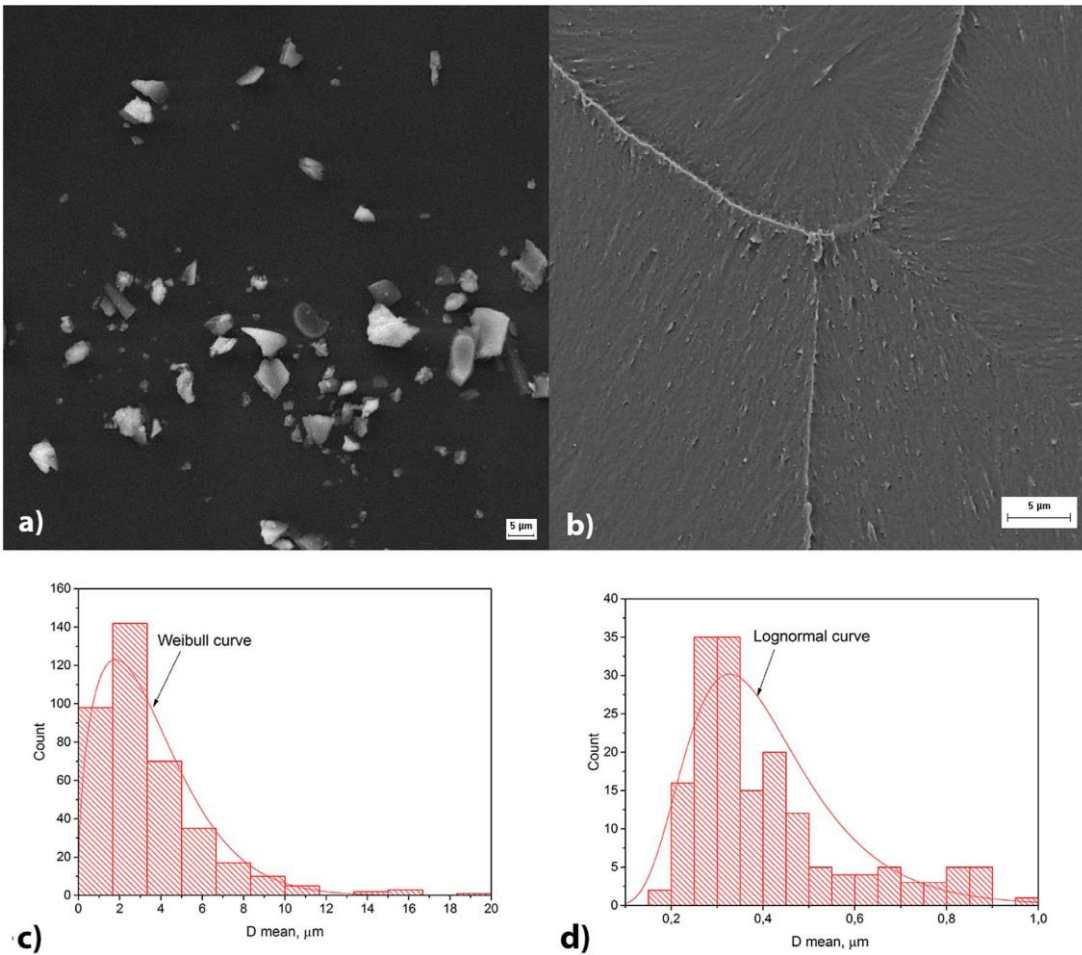


Figure 17 The FESEM micrographs of: a) agglomerated ferrous oxide doped alumina particles, b) composite having PMMA matrix and 3 wt. % of ferrous oxide doped alumina particles at 900 °C, c) distribution of the diameter of synthesized alumina particles sintered at 900 °C, d) distribution of the diameter of synthesized alumina particles dispersed in composites [68].

The results in pore volume and surface areas of the alumina-based particles and ferrous oxide doped alumina particles are given in Table 4.

The ferrous oxide doped alumina particles have a somewhat greater pore volume of 0.22 cm³/g that can be explained as the consequence of the increase in pore diameter with 5 nm of Al₂O₃ at 700 °C to 7 nm of ferrous oxide doped Al₂O₃ at 900 °C. Accordingly, the

surface area of ferrous oxide doped Al_2O_3 at $900\text{ }^\circ\text{C}$ is also affected. It can be concluded that the pores belong to the mesoporous on the basis of the obtained values. Transformation to the well-defined and long-range order in corundum (α phase) leads to the collapse of the porous structure characteristic of the low-temperature (transition) phases and the consequent diminishment of the particle specific surface area [47].

6.4 THE XRD ANALYSIS OF ALUMINA PARTICLES CRYSTAL STRUCTURE

The XRD diffractograms of the synthesized alumina-based particles after heat treatment at $700\text{ }^\circ\text{C}$, $800\text{ }^\circ\text{C}$ and $900\text{ }^\circ\text{C}$ are shown in Figure 18 and characteristic phases are marked.

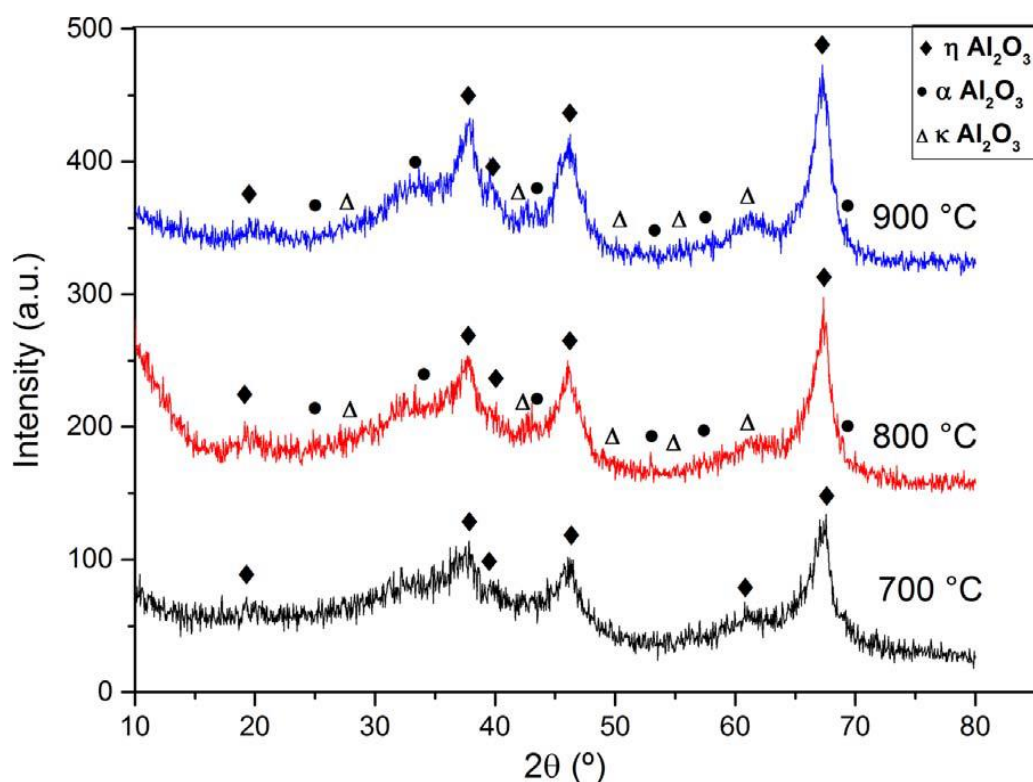


Figure 18 XRD of the synthesized alumina-based particles after heat treatment at $700\text{ }^\circ\text{C}$, $800\text{ }^\circ\text{C}$ and $900\text{ }^\circ\text{C}$ [68].

The dominant structure in the synthesized alumina-based particles sintered at $700\text{ }^\circ\text{C}$ is η – Al_2O_3 (PDF-2 77-0396). The phase present in the particles at $800\text{ }^\circ\text{C}$ are η – Al_2O_3 (PDF-2 77-0396), κ – Al_2O_3 (PDF-2 73-1199) and the small amount of α – Al_2O_3 (PDF-2 74-1081)

about 4 % which indicate that the crystallization of corundum is started at this temperature. The dominant phases in particles after heat treatment at 900 °C is η - Al_2O_3 (PDF-2 77-0396), κ - Al_2O_3 (PDF-2 73-1199) and α - Al_2O_3 (PDF-2 74-1081). The XRD patterns of the synthesized alumina-based particles doped with iron oxide after heat treatment at 700 °C, 800 °C and 900 °C are shown in Figure 19.

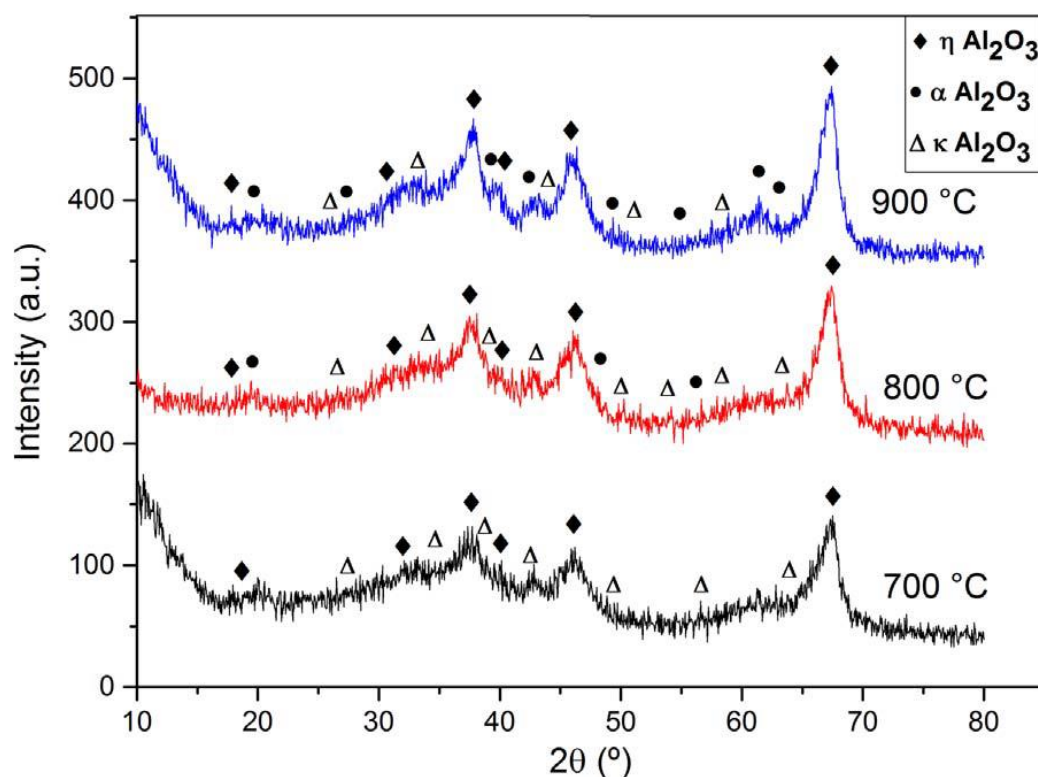


Figure 19 XRD of the synthesized ferrous oxide doped alumina particles after heat treatment at 700 °C, 800 °C and 900 °C [68].

The alumina-based precursor particles with the addition of FeCl_3 after heat treatment at 700 °C has η - Al_2O_3 (PDF-2 77-0396) and κ - Al_2O_3 (PDF-2 73-1199). The dominant phases in particles after heat treatment at 800 °C and 900 °C were η - Al_2O_3 (PDF-2 77-0396), κ - Al_2O_3 (PDF-2 73-1199) and α - Al_2O_3 (PDF-2 74-1081). The addition of ferrous oxide eases the formation of corundum and in particles calcinated at 900 °C presence of corundum is about 25.5%.

Table 5 Amount of crystalline phases of alumina particles at different temperature of sintering [68].

Particles	η – phase (%)	κ – phase (%)	α – phase (%)
Al ₂ O ₃ 700 °C	100.0	-	-
Al ₂ O ₃ 800 °C	53.0	43.0	4.0
Al ₂ O ₃ 900 °C	43.1	38.3	18.6
Al ₂ O ₃ Fe 700 °C	52.9	47.1	-
Al ₂ O ₃ Fe 800 °C	42.2	45.4	12.4
Al ₂ O ₃ Fe 900 °C	39.4	35.1	25.5

During high temperature treatment of alumina precursors, various transition alumina as may be formed before reaching the most stable α -Al₂O₃ phase. The polymorphism of alumina depends on the oxygen sublattice structure and distribution of aluminum ions in tetrahedral and octahedral interstitial sites [69]. Oxygen sublattice of α -Al₂O₃ is hexagonal close-packed crystal structure; while transition alumina (γ , η , κ , θ) has a face-centered cubic crystal structure that determine the density and the properties of each. α -Al₂O₃ has high hardness and it is mostly used to achieve reinforcement effect [63, 64]. γ -Al₂O₃ with loosely crystal structure has a higher specific surface area than α -Al₂O₃ [65] and exhibits high absorptive performance [70]. It was shown that the transitional aluminas improve mostly the toughness of the composite as their interactions with the matrix contribute to the possibility to absorb energy [71]. Higher amount of α phase of Al₂O₃ Fe may enable a greater amount of a reinforcing effect than Al₂O₃ m particles, especially when the hardness of the material is concerned. The presence of transition aluminas in both of the sintered particles ensures the high specific surface area compared to the commercial α -Al₂O₃ that will ensure the establishment of effective contact with the polymer matrix.

6.5 STRUCTURE CHARACTERIZATION VIA FTIR SPECTROSCOPY FOR ALUMINA BASED PARTICLES AT DIFFERENT TEMPERATURES

The FTIR spectra of alumina particles sintered at different temperature are shown in Figure 20. The characteristic peaks of alumina particles observed in 3000 – 3500 cm^{-1} can be assigned to O-H groups. The peaks at 822, 763 and 628 cm^{-1} are attributed to the Al – O bonds [72] that are supposed to arise from a pseudo boehmite structure [64]. Frequencies are reported as 630 cm^{-1} for the Al–O stretching mode and at 763 cm^{-1} for the torsional mode [71]. The FTIR spectrum of alumina fillers shows the main differences in the bands centered at ≈ 600 and ≈ 800 cm^{-1} , assigned to the vibrations of the Al–O bonds in tetrahedral and octahedral environments, respectively, which suggested the structural changes of synthesized alumina fillers.

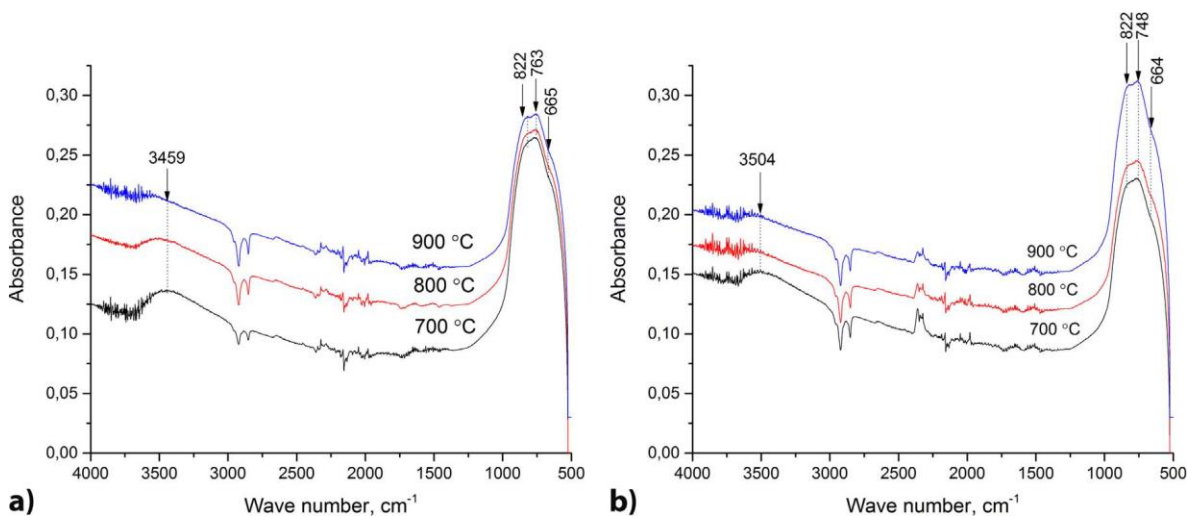


Figure 20 Comparison of FTIR spectra for alumina particles at different calcination temperatures: a) synthesized alumina particles, b) ferrous oxide doped alumina particles [63].

6.6 STRUCTURE CHARACTERIZATION VIA FTIR SPECTROSCOPY FOR PMMA/DMI/AL₂O₃ COMPOSITES

When the metal oxide surface is exposed to ambient air, the surface reacts with water to produce surface hydroxyl groups that can be easily detected by ATR-FTIR (denoted as Al₂O₃-OH) [73]. Spectra for Al₂O₃ n, Al₂O₃ m and Al₂O₃ Fe fillers (Figure 20a) showed the

changes in the intensities of absorption bands at 3300 cm^{-1} that were attributed to the presence of the O–H groups [74]. The presence of hydroxyl groups is additionally supported by the weak-intensity absorption band at $1636/1639\text{ cm}^{-1}$, related to the OH vibrational bending mode. The peak intensity of O–H groups for $\text{Al}_2\text{O}_3/\text{Fe}$ indicated that these groups were present in a greater content on the surface than on the surface of $\text{Al}_2\text{O}_3/\text{n}$ and $\text{Al}_2\text{O}_3/\text{m}$. The function of these groups was the establishing of better intermolecular interactions with the PMMA/DMI matrix as presented in Figure 22. Polar ester groups of PMMA/DMI have a dipole that participates in establishing of dipole/dipole interactions with the particles. An introduction of DMI into the system increases the number of polar sites favorable for dipole formation. The higher amount of interactions is achieved, the better dispersion of particles is reached and the interface adhesion particle/matrix is better. Therefore, when a large number of interactions are present in the system, then a uniform reinforcement dispersion is provided so as the better load transfer from the matrix to the particles.

The ethylene C-H stretch bands for PMMA, PMMA/DMI and composites at 2850 , 2950 and 3000 cm^{-1} were sharp and strong [75] and were found in similar positions for all composites, Figure 21b. The spectrum of PMMA, PMMA/DMI and composite displays a typical carbonyl C=O stretch band ($\sim 1732\text{ cm}^{-1}$). Other bands present in the spectrum of PMMA are a doublet of medium intensity in the region $1500\text{--}1425\text{ cm}^{-1}$, a medium-to-strong band $\sim 1148\text{ cm}^{-1}$ and a medium-intensity band at 750 cm^{-1} [76]. The characteristic peak for PMMA at 1352 cm^{-1} appeared due to O–CH₃ deformation vibration. Other two characteristic peaks at ($1140\text{--}1160\text{ cm}^{-1}$) relate to the methyl ester groups of PMMA. No significant differences were noticed for matrix spectra by the addition of DMI that were expected due to the low weight fraction and the similarity of PMMA and DMI structure. The presence of the residual monomer MMA or DMI may be evidenced by the appearance of the skeletal C=C double bond vibrations at 1637 cm^{-1} . This peak also overlaps with the OH vibrational bending mode (1637 cm^{-1}), so the estimation of the peak height ratio was taken into consideration, Table 6. The normalization of C=C peak height was done by both C=O (1732 cm^{-1}) and C–H (2950 cm^{-1}) peak heights. Sharp drop of the value obtained from the C=C/C=O ratio of PMMA/DMI matrix was due to the introduction of higher amount of C=O by double methyl ester groups of DMI. The

increase of C=C/C=O ratio by particle introduction was mainly due to the presence of hydroxyl groups that contribute to the increase in 1637 cm^{-1} peak height. Since the Al_2O_3 Fe particles have the highest amount of surface hydroxyl groups, but the lowest C=C/C=O ratio it may be concluded that the composite PMMA/DMI/ Al_2O_3 Fe has the lowest residual monomer content. Clearer picture can be seen when considering the C=C/C-H ratio. The values suggest the similar trend as in C=C/C=O ratio, but with different phenomenon operative. The ratio of H protons from double over single bonds is twice lower for DMI molecule than for MMA. This means that the main contribution to C=C/C-H ratio of the PMMA/DMI sample was given by the MMA presence which is also evidenced by a decrease of C=C/C-H ratio. Similar to the previous ratio, the values for composites are increased due to the presence of hydroxyl groups. A significant drop of C=C/C-H ratio value was observed for PMMA/DMI/ Al_2O_3 Fe suggesting that Al_2O_3 Fe particles are the most effective in reduction of MMA monomer content.

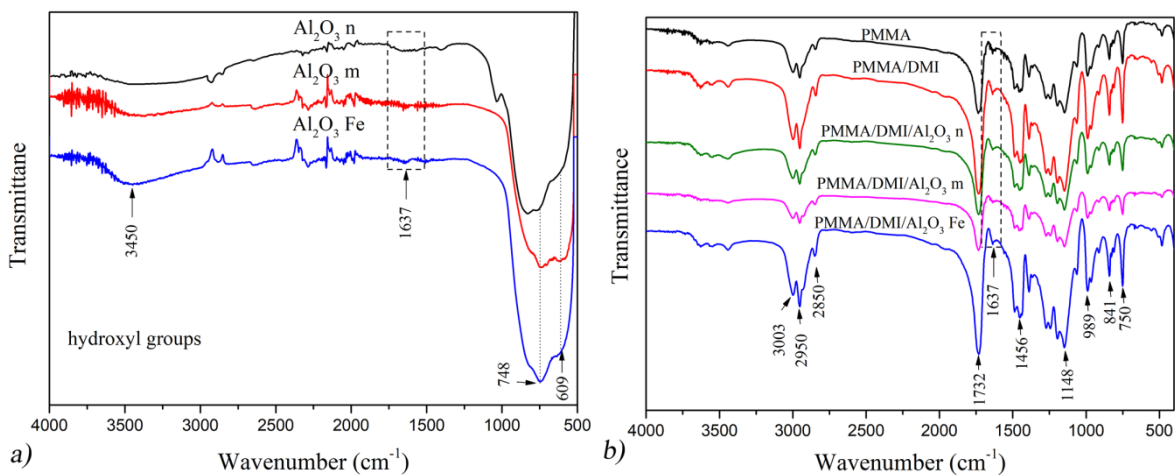


Figure 21 FTIR spectra of: a) alumina based fillers: Al_2O_3 n, Al_2O_3 m, Al_2O_3 Fe; b) comparative spectra of pure PMMA, PMMA modified with dimethyl itaconate (PMMA/DMI), and composites with 5 wt. % of particles in PMMA/DMI dental matrix [66].

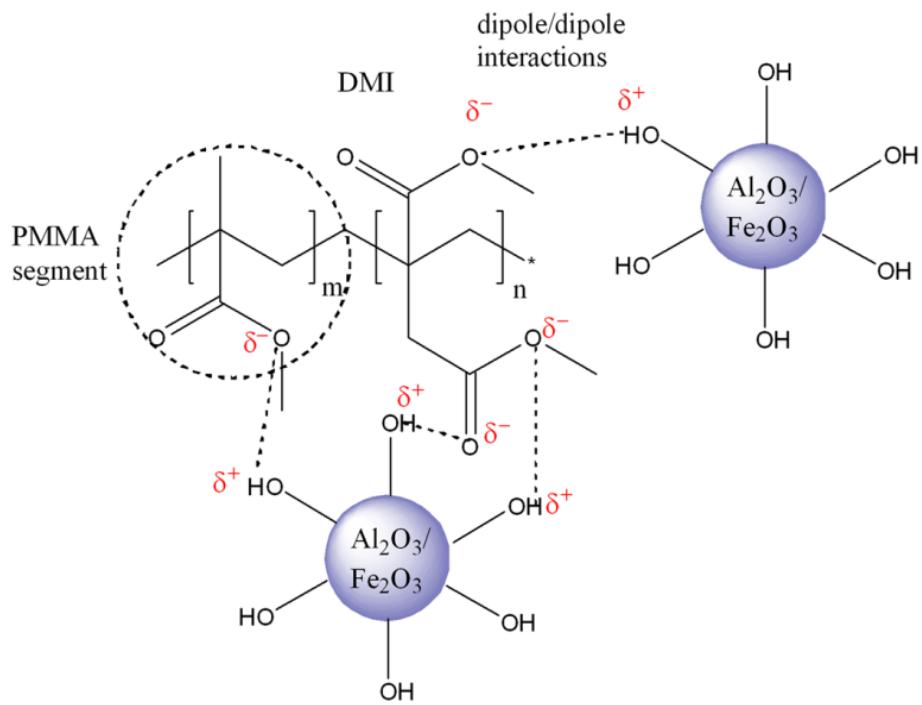


Figure 22 Schematic representation of increased dipole/dipole interactions by introducing DMI in polymer matrix [66].

Table 6 Estimation of the residual monomer by FTIR spectroscopy by a C=C bond content

[66].

Sample	Particle wt. %	C=C/C=O (1637/1732 cm⁻¹)	C=C/C-H (1637/2950 cm⁻¹)
PMMA	-	0.171	0.351
PMMA/DMI	-	0.119	0.204
PMMA/DMI/Al ₂ O ₃ n	5	0.150	0.251
PMMA/DMI/Al ₂ O ₃ m	5	0.130	0.242
PMMA/DMI/Al ₂ O ₃ Fe	5	0.128	0.201

6.7 MICRO HARDNESS MEASUREMENTS OF PMMA COMPOSITES

Micrograph of micro Vickers indentation for composites with 3 wt. % of composites with alumina-based particles are shown in Figure 23.

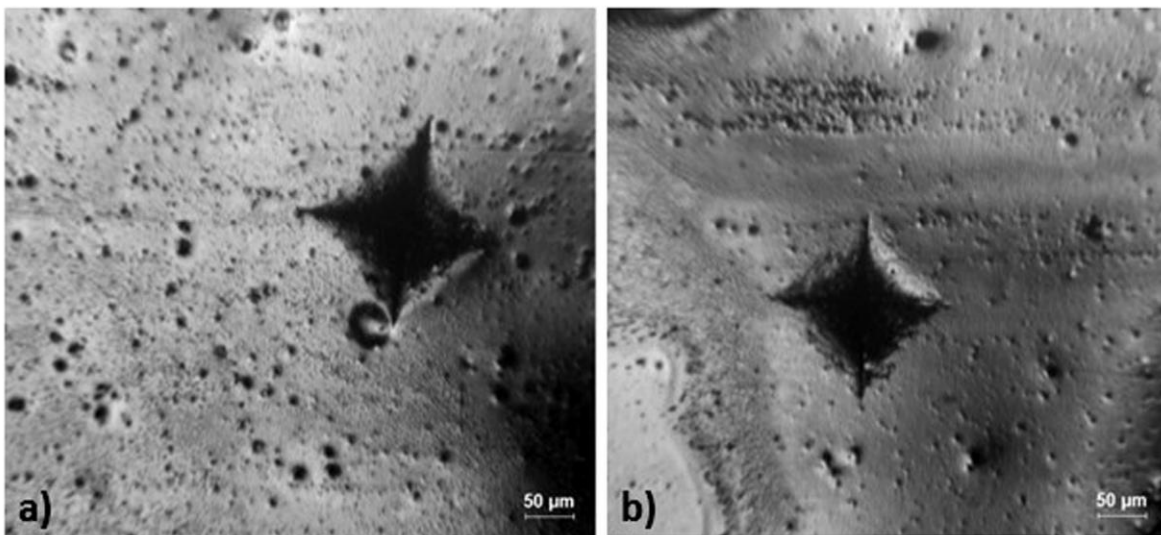


Figure 23 Micrograph of micro Vickers indentation for composites: a) with 3 wt. % of synthesized alumina particles sintered at 700 °C, b) with 3 wt. % of the ferrous oxide doped alumina particles sintered at 700 °C [68].

The matrix material, PMMA, has a micro hardness of 0.2373 GPa. A micro hardness of composites with addition of 3 wt. % of alumina is presented in Figure 24. A micro hardness of composites with the addition of 3 wt. % of the synthesized alumina particles increases for 26 % in the composite made with particles sintered at 700 °C, up to 54 % for the composite prepared using the particles sintered at 900 °C compared to the pure matrix material. But

composites with addition of 3 wt. % of the synthesized ferrous oxide doped alumina particles had the higher micro hardness improvement from 36 %, when the composite is prepared using the particles sintered at 700 °C, up to 99 % for the composite prepared using particles sintered at 900 °C compared to the pure matrix material.

The improvement of hardness is more important when the ferrous oxide doped particles were used in the composite. Those results indicate that the chemical composition as well as the sintering temperature of reinforcing particles influence the mechanical properties of the composite.

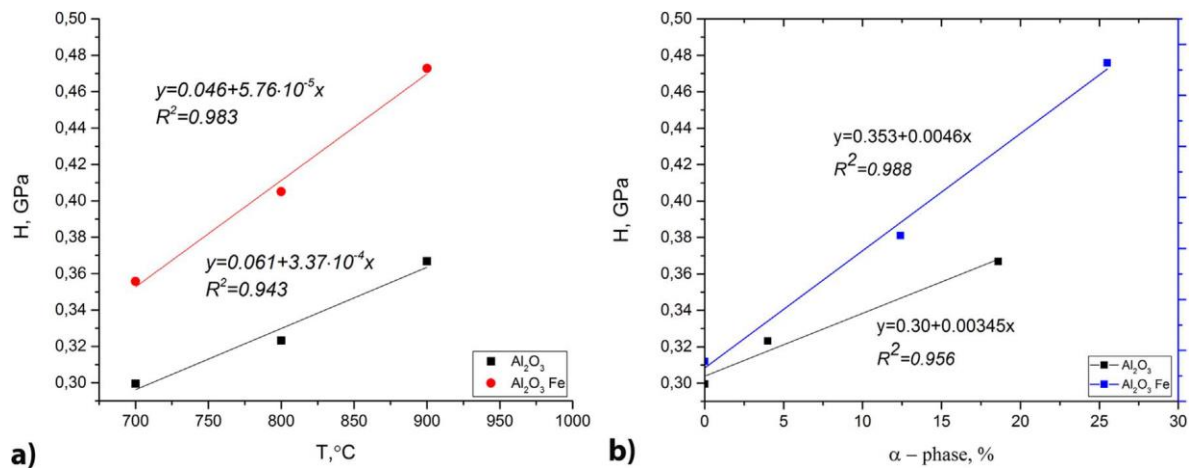


Figure 24 a) Micro hardness of composites vs. calcination temperature and b) micro hardness of composites vs. amount of α -phase [68].

When the hardness results are compared to the observed crystal structure in the ceramic reinforcement the comparison of the hardness values was related to the presence of corundum in the material and linear correlation to the corundum content to the hardness of the composite

is observed. The values of the R^2 factor are similar to the dependence of hardness and temperature of sintering and dependence of hardness and amount of α – phase in particles.

6.8 TENSILE TESTING FOR PMMA COMPOSITE

Tensile testing represents the most demanding way to test the composite material. This test is applied in order to see how the material behaves in the less favorable way of load application. On the other hand when the material is in the exploitation conditions it could be seen, by appropriate mathematical modelling, that in some parts of the material, denture for example, is exposed to tensile stress.

Tensile testing is performed in order to obtain the modulus and strength of composites depending on the sort of reinforcement used. All the samples have the same amount of the ceramic reinforcement of 3 wt. %. The values of tensile strength and modulus of elasticity (E) are shown in Figure 25.

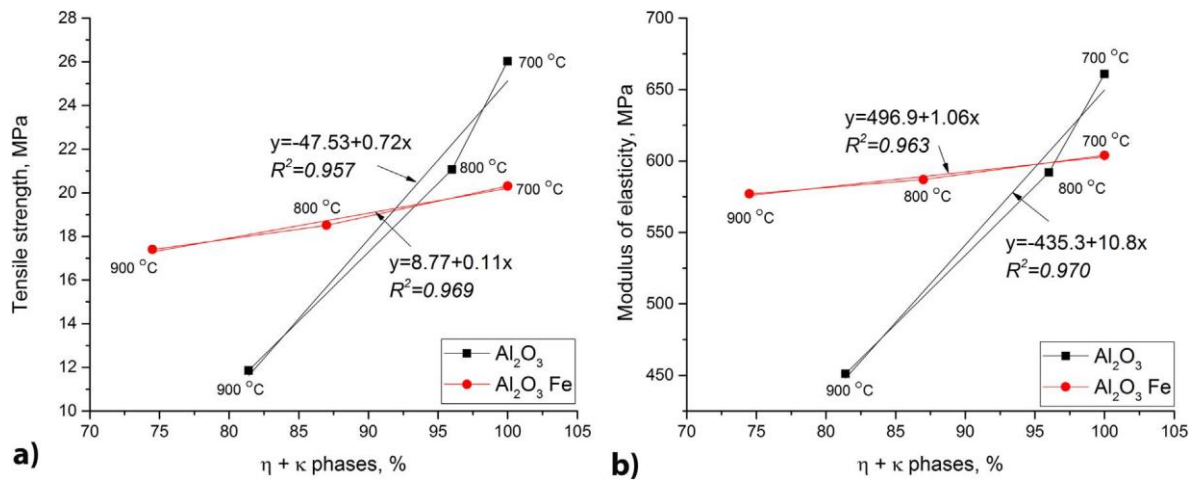


Figure 25 Dependence: a) tensile properties of PMMA matrix and obtained composites vs. amount of $\eta + \kappa$ phases, b) the values of modulus of elasticity (E) vs. amount of $\eta + \kappa$ phases [68].

Figure 25 shows that the amount of η and κ phases in the particles could be related to the mechanical properties of the composite. There is a linear dependence of a tensile strength of the composite on the fraction of the η and κ phase sum in synthesized alumina particles and ferrous oxide doped alumina particles, Figure 25a. The dependence of the Yung's modulus of elasticity on the amount of the η and κ phases is also linear in synthesized alumina particles and ferrous oxide doped alumina particles. The values of the R^2 are higher in composite with synthesized alumina particles, Figure 25b. The improvement in tensile strength is much more important for the materials where the reinforcement is composed of the particles sintered at 700 °C than that sintered at 900 °C especially for the pure alumina particles. This fact was correlated to the content of η and κ phases in the particles. The same analysis was done for the composites that contained the ferrous oxide doped particles and for those particles the increase in modulus of elasticity was much less sensitive to the content of those phases. The

best-reinforcing action, in terms of tensile properties, was obtained using the particles that are entirely composed of alumina $\eta + \kappa$ phases.

The influence of the crystal structure on the tensile strengths has the same trend as that for the modulus of elasticity. The best performance is obtained using the pure alumina particles sintered at 700 °C. The improvement obtained using ferrous oxide doped particles is not very dependent on the crystal structure of the reinforcement.

6.9 MECHANICAL PROPERTIES OF DENTAL PMMA/DMI/AL₂O₃ COMPOSITES

A series of PMMA/DMI/Al₂O₃ composite materials were prepared. Structural and morphological characterization was performed in order to determine the influence of alumina crystalline structure, the difference in chemical composition and size on interactions with the polymer matrix and therefore on material properties. This approach was a useful tool for discussion of the structure/property relationship study of composites, and helped in an analysis of the compatibility between the reinforcement and the matrix.

Mechanical testing was performed in order to investigate the influence of geometry and amount of alumina particles on tensile characteristics of the obtained composites. The values of tensile stress at break (σ_t), elongation at break (ϵ_t), and tensile modulus (E_t) are shown in Table 7. The addition of DMI to the matrix slightly increased tensile strength and modulus of elasticity, but also reduced elongation at break, indicating the increased rigidity of the matrix. Such results suggested that the incorporation of higher amount of pendant groups by

DMI disturbed the regular packing of polymer chains causing micro-defects in polymer structure that resulted in earlier failure (lower elongation at break) of PMMA/DMI samples.

6.9.1 Tensile testing of PMMA/DMI/Al₂O₃

Results of tensile tests indicate that incorporation of 1 wt. % of Al₂O₃ Fe caused significant increase of σ_t , ε_t and E_t (37.5, 9.4, 18.8%, respectively) relative to the PMMA/DMI matrix.

Noticed an increase may be prescribed to the effective dispersion of Al₂O₃ Fe particles due to establishing of higher amount of intermolecular (dipol/dipol) interactions between surface hydroxyl groups of particles and polar pendant groups of PMMA/DMI matrix, Figure 21.

Figure 22 shows the increased amount of established interactions, which enabled effective dispersion of reinforcing particles and thus the improvements of mechanical properties of PMMA/DMI/Al₂O₃ Fe composites. Particles with lower amount of surface hydroxyl groups (Al₂O₃ n) tend to form aggregates and thus to deteriorate mechanical properties. The advantage of the use of Al₂O₃ Fe in improving mechanical properties compared to the Al₂O₃ m lies in the crystal structure with higher content of α -Al₂O₃ resulting in particles with better reinforcing effect. Al₂O₃ Fe particles having the transition alumina composition exhibit also adsorption capacity of monomer that fill the cavities on the particle surface and establish mechanical anchors after polymerization. The presence of transition alumina structures in those particles increases the interface connecting the particle and the matrix and the loads are transferred more efficiently to the filler particles resulting in increased tensile strength.

Table 7 Tensile properties of PMMA matrix and obtained composites [66].

Sample	Particle wt. %	Tensile strength (σ_t), MPa	Elongation at break (ϵ_t), %	Modulus of elasticity (E_t), MPa
PMMA	0	38.7	10.61	593.6
PMMA/DMI	0	39.5	7.88	800.0
PMMA/DMI/Al ₂ O ₃ m	1	32.4	7.27	658.8
	3	36.6	8.73	657.6
	5	34.0	7.04	792.8
PMMA/DMI/Al ₂ O ₃ n	1	39.9	7.31	725.4
	3	29.3	6.75	685.2
	5	31.8	6.71	791.6
PMMA/DMI/Al ₂ O ₃ Fe	1	54.3	8.62	950.5
	3	37.4	6.85	940.7
	5	30.8	6.54	724.5

6.9.2 Toughness testing of PMMA/DMI/Al₂O₃

Energy absorbed per volume of material (toughness) is obtained from numerical integration of data in a measured stress-strain experiment, Figure 26. The highest energy absorption was found for composite PMMA/DMI/1 wt. % Al₂O₃ Fe that was increased to 127% and 36.3% compare to PMMA/DMI and PMMA, respectively. The higher filler loading caused a decrease in toughness of composite because of the formation of particle aggregation and defects in microstructure.

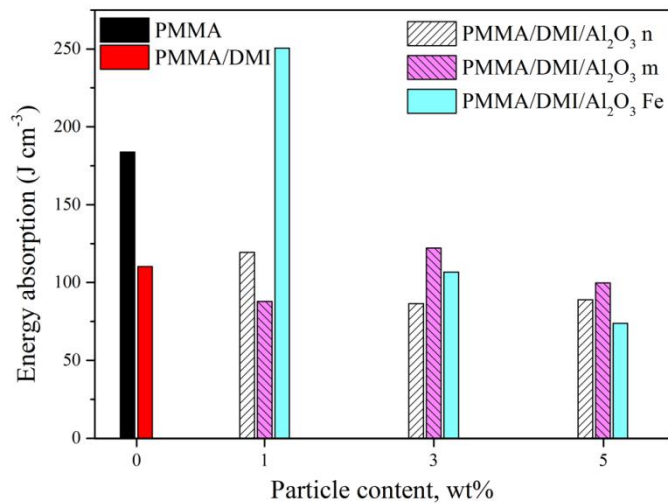


Figure 26 Toughness of dental composites represented as energy absorption (area under tensile stress-strain diagram) versus particle type and content [66].

6.9.3 Micro Vickers hardness of PMMA/DMI/Al₂O₃

Micro Vickers hardness (HV) measurements were performed in order to determine hardness as a measure of surface resistance to wear, cutting, and scratching that increase applicability of PMMA/DMI dental composites. According to the hardness variations under low loads it is possible to obtain information about filler aggregation, identification of composite constituents and characterization of microstructure gradients. The average values of indent diagonals, d , were calculated from six independent measurements of three indents, and calculated according to eq 1. The results of Micro Vickers hardness testing are presented in Table 8. Standard deviation as a measure of HV value variation demonstrated the aggregation of Al₂O₃ m and Al₂O₃ n particles at higher particle content. The composite reinforced with alumina particles doped with iron oxide (Al₂O₃ Fe) showed the highest hardness value. This

result was expected since the Al₂O₃ Fe particles consist of the high value of α -Al₂O₃ content. The typical indents in the composite material are given in Figure 27, which is showing improvement of indentation resistance of composites compared to the polymer matrix PMMA/DMI alone.

Table 8 Micro Vickers hardness of PMMA and PMMA/IT matrix and composites reinforced with alumina based particles [66].

Sample	Particle wt. %	HV
PMMA	-	21.3 ± 1.0
PMMA/DMI	-	28.7 ± 1.2
PMMA/DMI/Al ₂ O ₃ m	1	26.0 ± 0.5
	3	28.2 ± 1.2
	5	32.5 ± 2.7
PMMA/DMI/Al ₂ O ₃ n	1	27.1 ± 1.1
	3	30.1 ± 2.4
	5	29.5 ± 1.0
PMMA/DMI/Al ₂ O ₃ Fe	1	32.6 ± 1.3
	3	39.4 ± 1.1
	5	37.4 ± 1.5

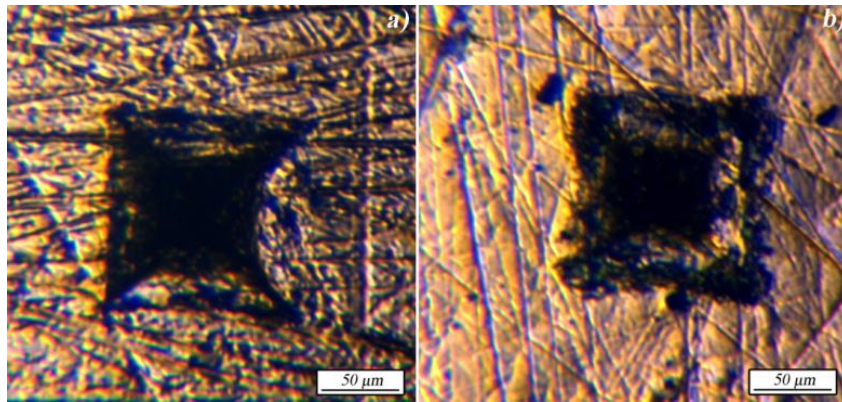


Figure 27 *Optical micrographs showing indents after Micro Vickers hardness test of: a) PMMA/DMI matrix and b) PMMA/DMI/3 wt. % Al_2O_3 Fe [66].*

6.9.4 Controlled energy impact testing

The composites reinforced with synthesized alumina particles and the ferrous oxide doped alumina particles were tested. The obtained results gave the information about the behavior of the composite in the situation of impact induced by a sudden hit. The results are shown in Figure 28a. The dependence of the energy on $\eta+\kappa$ phase content obtained from impact test for samples with alumina-based reinforcement was shown in Figure 28b.

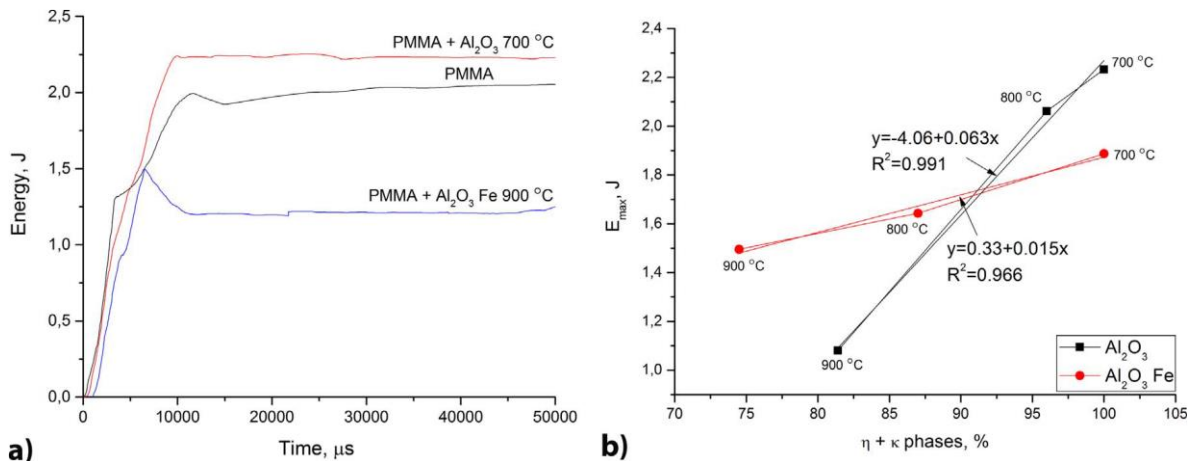


Figure 28 a) Controlled energy impact testing of pure PMMA and composite with alumina particles, b) the energy– $\eta + \kappa$ phases curves obtained from impact test for samples with alumina based reinforcement [68].

The composite materials with synthesized alumina particles have higher toughness than composites with ferrous oxide doped alumina particles. In addition, the sintering temperature has a great influence on the toughness of the composite material. The synthesized alumina particles sintered at 700 °C have the highest toughness. This is due to the crystal structure, *i.e.* because there is no presence of corundum phase and η and κ were proved to improve tensile properties of the composite better. A hybrid composite with 1.5 wt. % of synthesized alumina particles at 700 °C, with the highest toughness, and 1.5 wt. % of the ferrous oxide doped alumina particles at 900 °C, with the highest hardness, were made. The energy value of hybrid composite is between the energy value of composite materials with synthesized alumina particles and the energy value of composite materials with ferrous oxide doped alumina particles as it can be seen from the diagram, Figure 28a. That proves that the addition of the ferrous oxide doped particles did not improve toughness of the composite. The

obtained result suggests that the properties could be predetermined and manipulated using different reinforcements for their preparation.

Different type of alumina and hydrated alumina particles were proven to have an influence on the flammability and thermal stability of the composites, but the mechanical properties were not investigated in that research [65]. Surface modifications of particles improved the miscibility of the reinforcement with the polymer matrix and they improved the mechanical and thermal properties with a very small amount of fillers in the composition [70]. It was discussed that the activation of the surface of the particles has an important role in the improvement of the composite properties. In the case of the particles studied in this paper, the mineralogical structure of the obtained particles differs due to calcination temperature and chemical composition. The corundum structure appears when sintering temperatures are higher and when the addition of ferrous oxide provokes its formation. The intermediate structures that were observed are known to have good activities in adsorption so their structure is open and enables the creation of the bonds with the matrix polymer. The improvement of the tensile properties is more influenced by the interface connections between the particles and the matrix. The hardness improvement is better with the addition of particles having more corundum in their structure as the corundum structure is harder than the intermediate phases and thus improves this property of the composite.

It can be seen that the best impact performance exhibited composite doped with 1 wt. % ferrous doped alumina particles, the same one that had the best improvement in tensile properties (tensile strength, elastic modulus, and energy absorption under tensile loading), Figure 29.

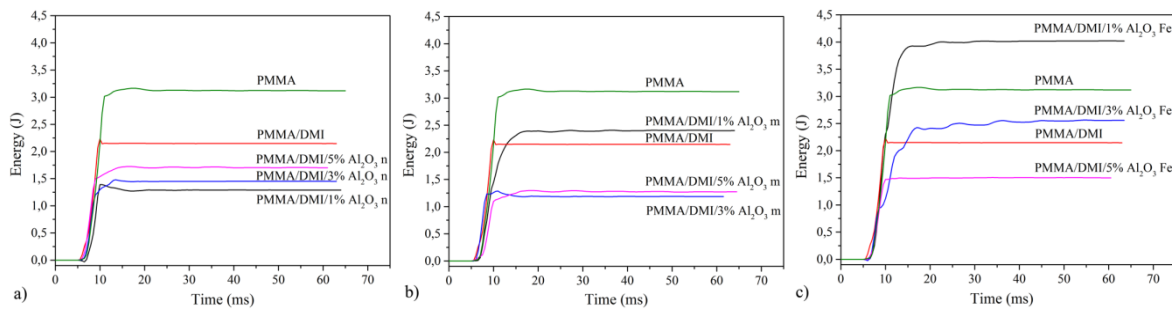


Figure 29 The energy–time curves obtained from impact test for samples with alumina based reinforcement: a) Al_2O_3 n, b) Al_2O_3 m, c) Al_2O_3 Fe [66].

Optical microscopy was employed in order to examine the type of composite failure under high-speed impact test, Figure 30.

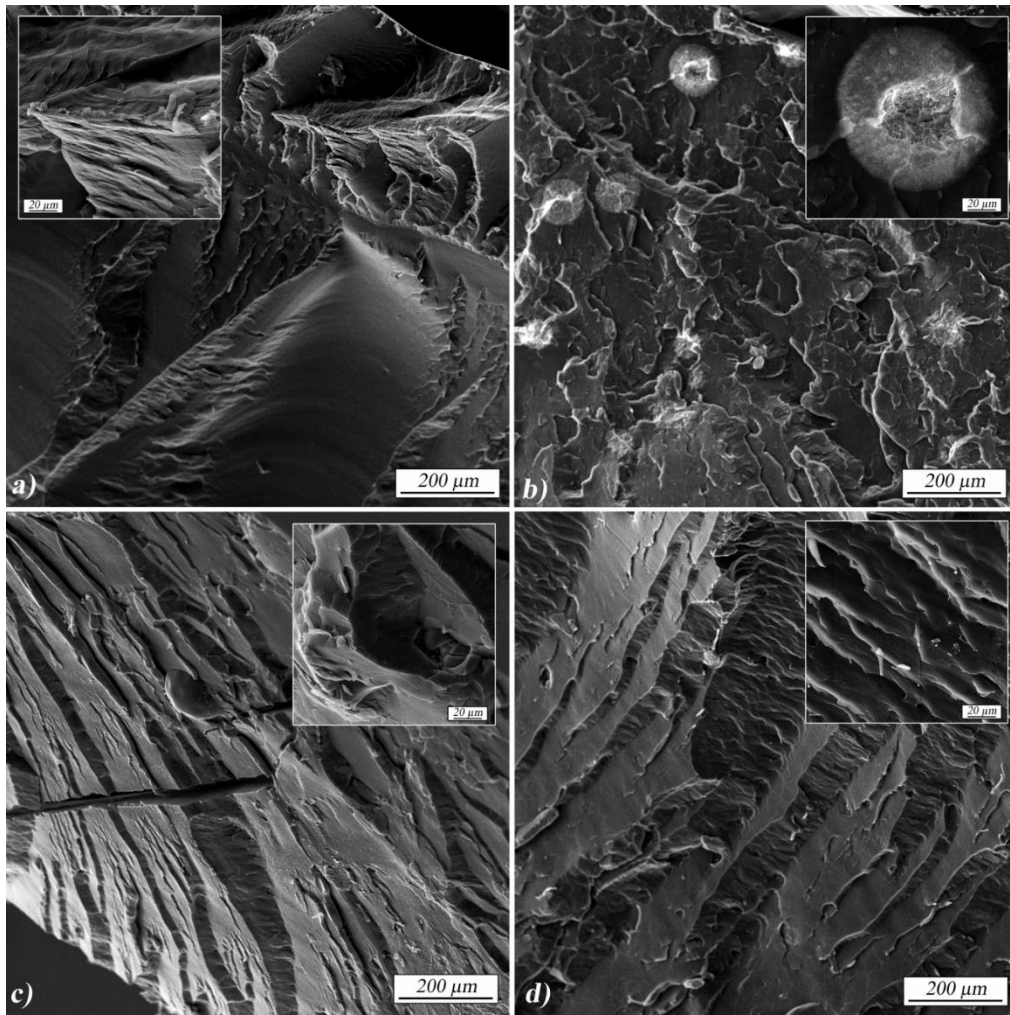


Figure 30 SEM images of the fracture surface of the specimens exposed to the controlled energy impact testing of: a) PMMA/DMI, and composites reinforced with: b) spherical nanoparticles – Al_2O_3 n, c) synthesized alumina particles – Al_2O_3 m, d) ferrous oxide doped alumina particles – Al_2O_3 Fe [66].

In all impact test experiments, the specimens exhibited a typical brittle fracture except of the composite reinforced with 3 wt. % of Al_2O_3 Fe that showed ductile failure. In ductile fracture, extensive plastic deformation (necking) takes place before fracture in tension. Diversity of information might be obtained about the composite strains during the examination of samples

through the polarized light on optical microscope. The appearance of optical strain in composites after impact test suggested the presence of a phenomenon called photo elasticity. Established effective interactions between the Al_2O_3 Fe fillers result in a higher strain while resisting to high-speed impact.

The lower impact resistance of composites reinforced with Al_2O_3 n and Al_2O_3 m may be attributed to the formation of aggregates of particles that were not able to disperse in the polymer matrix, which is obvious in Figure 31. These agglomerates act as a stress concentrator and represent a crack location. It could be noticed that aggregates did not act as a barrier for crack propagation since the crack spread across the spherical aggregate.

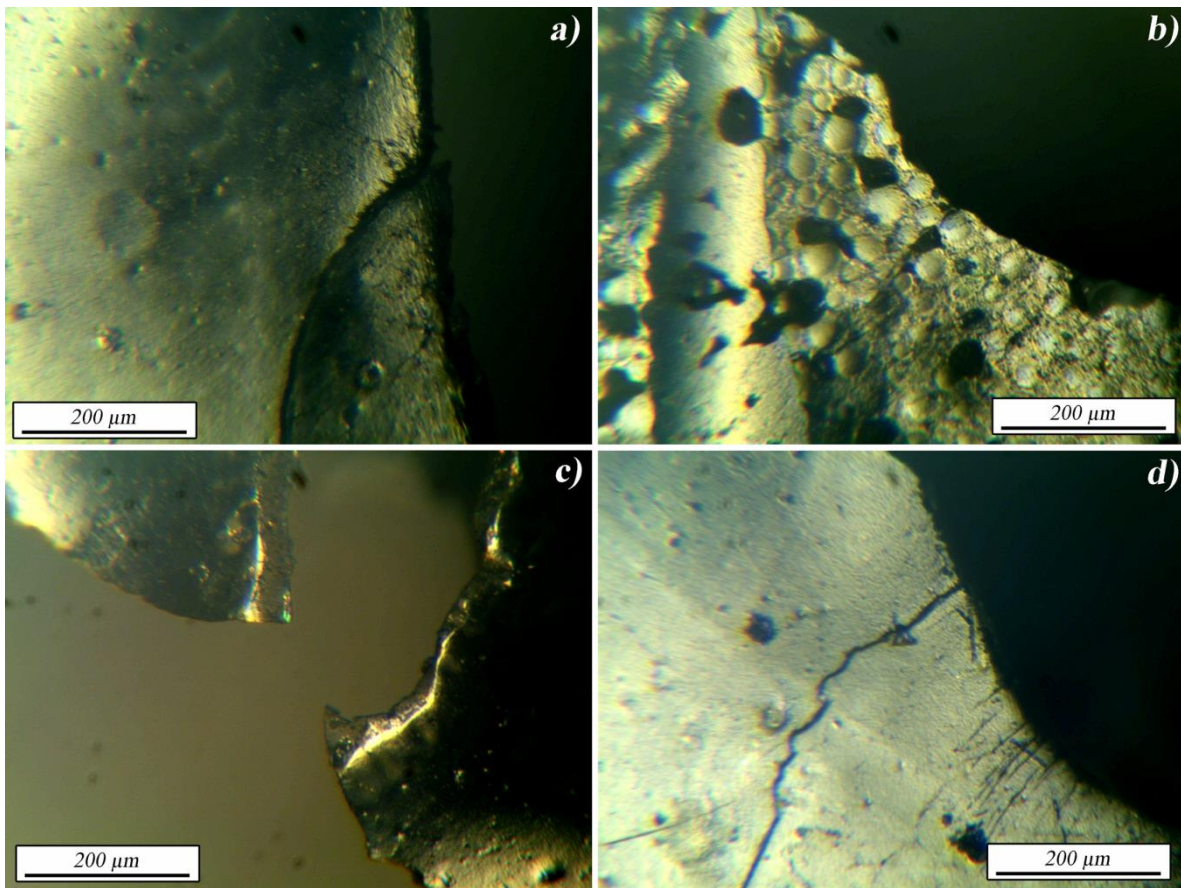


Figure 31 Optical micrographs with crossed nicols in a reflection mode showing the type of composite failure after impact testing and optical elasticity of: a) matrix PMMA/DMI and composites reinforced with 3 wt. %: b) Al_2O_3 n, c) Al_2O_3 Fe, and d) Al_2O_3 m [66].

6.10 RESIDUAL MONOMER DETERMINATION

Recently, many research studies were conducted in order to find the adequate replacement of MMA monomer. The aim of partial MMA replacement was the decrease of residual monomer. Due to the introduction of reinforcement into the PMMA/DMI matrix, it was important to determine the influence of the presence of fillers on residual monomer content.

The values of residual MMA, DMI and total residual monomer (TRM) content of the dental polymer matrix and the composite with the best mechanical performance (PMMA/DMI/Al₂O₃ Fe) are presented in Table 9. It can be noticed that the highest residual MMA content is present in the commercial dental PMMA material. The addition of DMI lowered the MMA content compared to the level in the commercial material to 37.3 % in modified PMMA/DMI copolymer. Significant results were observed in the PMMA/DMI/Al₂O₃ Fe composites. The addition of 5 wt. % Al₂O₃ Fe resulted in decrease of MMA (15.3%) and DMI (42.9%) content. Major and selective influence of the residual DMI content may be attributed to the surface absorption of more polar DMI (compared to MMA) on Al₂O₃ Fe surface. Al₂O₃ Fe may exhibit catalytic properties on copolymerization kinetics which can be confirmed by the decreased TRM content [77]. All materials synthesized in this study conform to the standard for denture base materials [27].

Table 9 Residual MMA, DMI and total residual monomer (TRM) content of the specimens (given as mean \pm standard deviation) for the dental materials [66].

Sample	Particle wt. %	Residual monomer		
		MMA, wt.%	DMI, wt.%	TRM, wt.%
PMMA	-	2.09 \pm 0.07	-	2.09 \pm 0.08
PMMA/DMI	-	1.31 \pm 0.04	1.56 \pm 0.06	2.87 \pm 0.10
PMMA/DMI/Al ₂ O ₃ Fe	1	1.14 \pm 0.03	1.42 \pm 0.05	2.56 \pm 0.09
	3	1.13 \pm 0.02	1.08 \pm 0.03	2.21 \pm 0.07
	5	1.11 \pm 0.02	0.89 \pm 0.01	2.00 \pm 0.04

The relation of chemical composition, crystallographic structure and mechanical properties of the composite are studied. The characterization of the filler particles is done using XRD technique that enables to determine the structure of the particles that could be further related to the mechanical properties of the composite material.

6.11 THE 3 POINT BENDING TEST

One could consider that it would be appropriate to test the material in the conditions that are very similar to those the material will withstand in exploitation. However, the material behavior does not depend only on the material composition but also on the specific situation encountered due to the anatomy of teeth, the 3-dimensional nature of jaw mechanics and the resulting stress in the material can be tensile stress. Testing of materials in tensile loading is typically considered most appropriate as it simulates the most challenging situation [78].

All specimens were compared to PMMA without any addition. The obtained results show that the addition of alumina nano particles are improving the modulus of elasticity of the composite as well as the flexural strength. In Figure 32 the comparison of modulus of elasticity of the prepared composite is compared to that of pure PMMA. The main problem with the addition of the diethyl itaconate to the matrix is the loss of mechanical properties compared to pure PMMA, and the addition of only 1 wt. % of the alumina spherical nano particles increase the values of modulus compared, and this increase is more important with the addition of more particles. The 3 point bending test is presented in Figure 32.

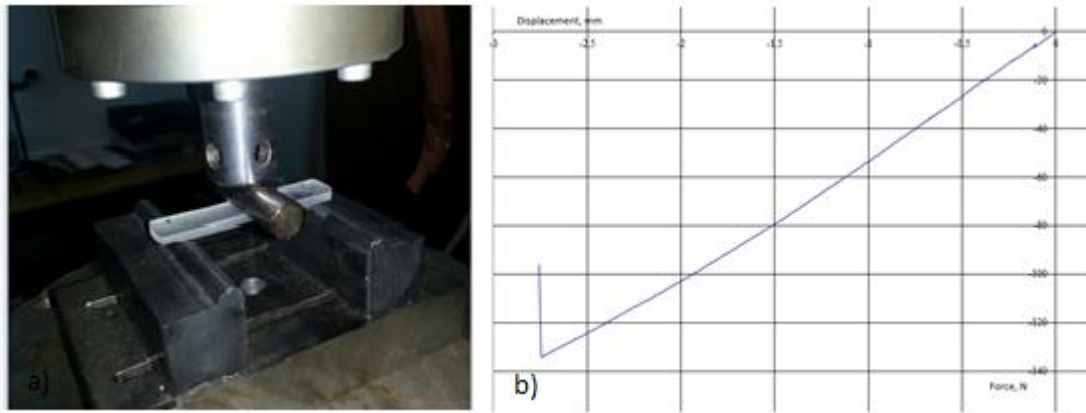


Figure 32 a) the 3 point bending testing machine with the specimen and b) a typical experimental diagram showing the displacement versus force for the tested specimen.

Obtained force-displacement data can serve to calculate the modulus of elasticity and flexural strength according to the procedure previously described. The obtained data are presented in Table 10.

Table 10 The results of 3 point bending test.

Specimen description	Modulus of elasticity, MPa	Flexural strength, MPa
PMMA	533.7	43.3
PMMA+It 1% spherical particles	667.2	84.5
PMMA+It 3% spherical particles	811.1	66.3
PMMA+It 5% spherical particles	880.6	61.0
PMMA+It 1% ferrous oxide doped alumina particles	607.9	64.0
PMMA+It 3% ferrous oxide doped alumina particles	881.6	58.3
PMMA+It 5% ferrous oxide doped alumina particles	716.9	70.4

The flexural strength also increases the flexural strength compared to the pure PMMA. The improvement is the largest with only 1 wt. % of spherical nano particles and addition of 3 wt. % and 5 wt. % of alumina nano particles do not have a more positive impact to the flexural strength of the composite, Figure 33. The composite modulus of elasticity of PMMA composite with spherical nano particles compared to polymer is shown in Figure 34.

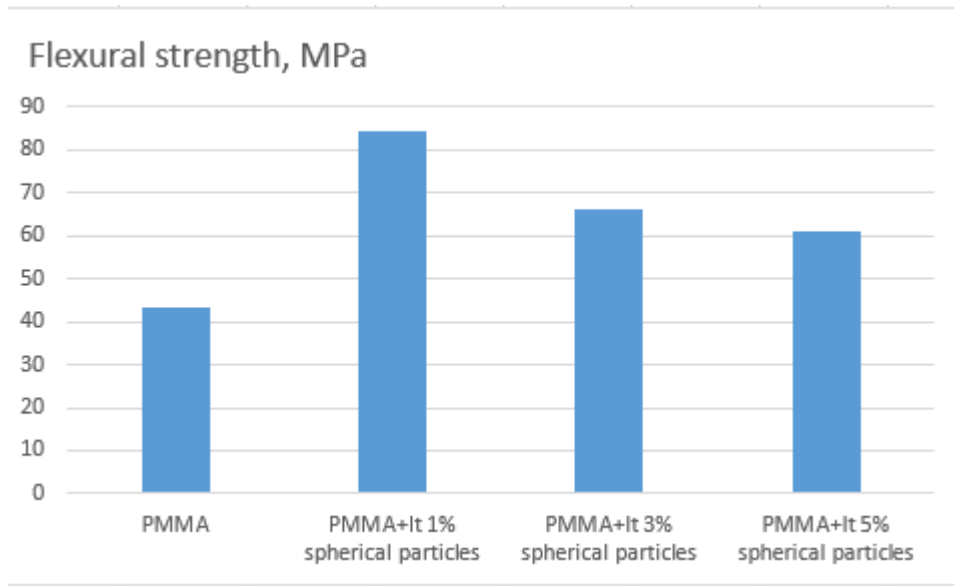


Figure 33 The flexural strength of the composite made with addition of alumina spherical nano particles to the matrix composed of PMMA and diethyl itaconate.

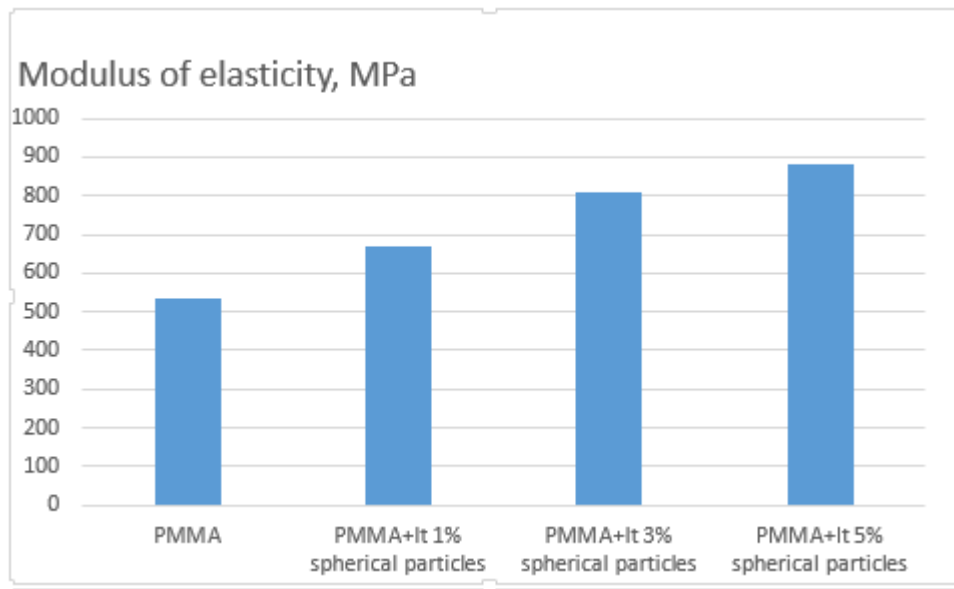


Figure 34 The comparison of composite modulus of elasticity compared to PMMA.

Addition of ferrous-doped alumina nano particles also improves both the flexural strength and the modulus of elasticity of the composite, Figure 35. As it can be seen in Figure 35 35

and Figure 36 the best performance is obtained with the composite having 3 wt. % ferrous oxide doped alumina particles, but this specimen has slightly lower flexural strength as compared to the composite having 1 wt. % and 5 wt. % of particles added.

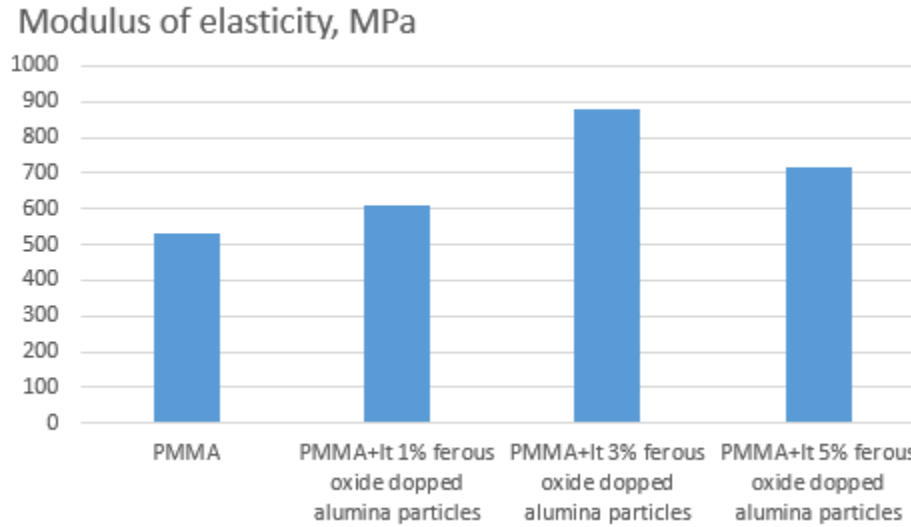


Figure 35 Modulus of elasticity of composites with ferrous oxide doped alumina particles compared to pure PMMA.

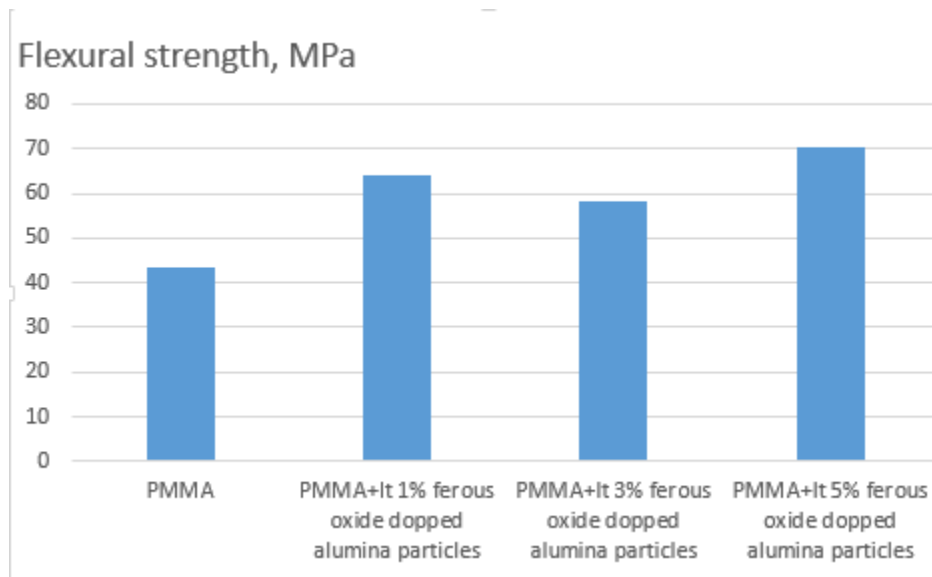


Figure 36 Flexural strength of ferrous oxide doped alumina particles compared to pure PMMA.

7 CONCLUSION

The composites for dental applications were examined with the aim to obtain the material having better biocompatibility and improved mechanical properties. The way to obtain this sort of a material was done using a modified matrix material consisting of PMMA modified using the ethyl itaconate. The obtained copolymer was used as a matrix for the new material. Mechanical properties of the matrix were improved using different alumina based particles synthesized using the sol-gel technique and modifying the crystal structure using different calcination temperatures.

Two types of alumina-based particles with different chemical compositions were heat treated at three different temperatures resulting in different crystalline structures. Composites having PMMA as a matrix polymer with addition of synthesized alumina-based particles were prepared. It was proved that different crystal structures and calcination temperature affect mechanical properties of the material. The addition of ferrous oxide affected the production of a higher amount of α -phase in particles with an increase in sintering temperature. The alumina particles having high alpha phase content improved the hardness of the material from 36% to 99% compared to the polymer. However, η and κ phases had more influence on tensile strength, Young's modulus of elasticity and toughness improvements.

The high-speed impact test was used to compare the behavior of synthesized composite materials in the situation of high-speed impact. Testing the impact of composites containing synthesized alumina particles at 700 °C showed that the particles improved the resistance to the high-speed impact. The use of ferrous-doped alumina particles gave the low performance in the impact testing. The energy value of the hybrid composite was between the energy value of composite materials with synthesized alumina particles and the energy value of composite materials with ferrous oxide doped alumina particles. This showed that properties of the material can be controlled depending on whether a material with better hardness or better toughness is desired.

PMMA is one of the most important materials that has a broad use in the dentistry as well as in the medical applications. The main problem when using this polymer is the reduction of the residual monomer and decreasing the quantity of monomer present in the material improves the biocompatibility of the material. The addition of diethyl itaconate to the preparation of PMMA results in a remarkable reduction of the residual monomer in the composition, but at the same time, it decreases some mechanical properties of the material. Composite materials are enabling the improvement of the mechanical properties of the polymers in order to be able to bear part of the load applied to the composite and thus small addition of particles, when they are of sub micrometer size improves the mechanical properties of the material.

In this paper, flexural strength was measured for composites having the PMMA matrix with the addition of dimethyl itaconate. The filler materials were aluminum-oxide spherical particles and ferrous oxide doped aluminum-oxide particles. The results are showing the significant improvement with the addition of both spherical alumina nano particles as well as the addition of ferrous oxide doped alumina nanoparticles. The obtained materials exhibited both improvements in measured modulus of elasticity as well as improvements in flexural strength. The increase of the quantity of added alumina spherical nano particles is resulting in improvements of modulus of elasticity and at the same time the improvements in flexural strength remain stable. Addition of ferrous oxide doped alumina nanoparticles have the best improvement in measured modulus of elasticity with the addition of 3 wt. % of those particles. Flexural strength is better than in pure PMMA but does not change significantly with the addition of bigger quantities of particles to the composite.

The specimens were tested using the high-speed impact tester and it was shown that all specimens have improved resistance to impact; the best performance has the composite doped with 3 wt. % of ferrous oxide doped alumina particles.

All the results are leading to the production of a composite material having determined mechanical properties and achieving lower amount of a monomer in the composite. The addition of ferrous oxide doped particles into the copolymer matrix gave the material having lower residual monomer level and improved mechanical properties that can be tuned by the appropriate selection of the reinforcement.

8 REFERENCE

- [1] <https://www.britannica.com/biography/Rowland-Hill-British-preacher>
- [2] <http://www.deutsches-kunststoff-museum.de/rund-um-kunststoff/erfinder/otto-roehm/>
- [3] J.F. McCabe, R.M. Basker, Tissue sensitivity to acrylic resin. A method of measuring the residual monomer content and its clinical application, *British Dental Journal*, 140 (1976) 347-350.
- [4] C.Y.K. Lung, B.W. Darvell, Minimization of the inevitable residual monomer in denture base acrylic, *Dental Materials*, 21 (2005) 1119-1128.
- [5] D.C. Smith, The acrylic denture base-mechanical evaluation of dental poly(methylmethacrylate), *British Dental Journal*, 111 (1961) 9-17.
- [6] A. Moshaverinia, N. Roohpour, S. Ansari, M. Moshaverinia, S. Schricker, J.A. Darr, I.U. Rehman, Effects of N-vinylpyrrolidone (NVP) containing polyelectrolytes on surface properties of conventional glass-ionomer cements (GIC), *Dental materials*, 25 (2009) 1240-1247.
- [7] A. Moshaverinia, S. Ansari, Z. Movasaghi, R.W. Billington, J.A. Darrhesham, I.U. Rehman, Modification of conventional glass-ionomer cements with N-vinylpyrrolidone containing polyacids, nano-hydroxy and fluoroapatite to improve mechanical properties, *Dental Materials*, 24 (2008) 1381-1390.
- [8] K. Kinashita, Formation of itaconic acid and mannite by a new filamentous fungus, *Journal of the Chemical Society*, 50 (1929) 583-593.
- [9] <http://omnexus.specialchem.com/selection-guide/polymethylmethacrylate-acrylic/applications-and-key-features>.
- [10] R.Q. Frazer, R.T. Byron, P.B. Osborne, K.P. West, PMMA: an essential material in medicine and dentistry, *Journal of Long-Term Effects of Medical Implants*, 15 (2005) 629-639.
- [11] T. Thielen, S. Maas, A. Zuerbes, D. Waldmann, J. Kelm, Mechanical material properties of polymethylmethacrylate (PMMA) for medical applications. *Materials Testing*, 51 (2009) 203-209.

- [12] ARKEMA <http://omnexus.specialchem.com/selection-guide/polymethylmethacrylate-acrylic/properties#content>.
- [13] D.F. Williams, On the mechanisms of biocompatibility, *Biomaterials*, 29 (2008) 2941-2953.
- [14] M.G. Steiger, M.L. Blumhoff, D. Mattanovich, M. Sauer, Biochemistry of microbial itaconic acid production, *Microbial Physiology and Metabolism*. 4 (2013) 1-5.
- [15] E. Geiser, S.K. Przybilla, A. Friedrich, W. Buckel, N. Wierckx, L.M. Blank, M. Bölker, *Ustilago maydis* produces itaconic acid via the unusual intermediate trans-aconitate, *Microbial Biotechnology*, 9 (2016) 116–126.
- [16] A. Michelucci, T. Cordes, J. Ghelfi, A. Pailot, N. Reiling, O. Goldmann, T. Binz, A. Wegner, A. Tallam, A. Rausell, M. Buttini, C.L. Linster, E. Medina, R. Balling, K. Hiller, Immune-responsive gene 1 protein links metabolism to immunity by catalyzing itaconic acid production, *Proceedings of the National Academy of Sciences*, 110 (2013) 7820–7825.
- [17] B. Axelsson, G. Nyquist, The leaching and biological effect of the residual monomer of methyl methacrylate, *Odontologisk Revy*, 27 (1962) 370-379.
- [18] J.K. Anusavice, Phillips' Science of Dental Materials, W B. Saunders Co., Philadelphia, PA, p. 176 (2003).
- [19] D.C. Smith, M.E. Bains, Residual monomer methyl methacrylate in the denture base and its relation to denture sore mouth, *British Dental Journal*, 98 (1955) 55-58.
- [20] B.E. Tate, Vinyl and Diene Monomers, Wiley-Interscience, New York, p. 205 (1979).
- [21] M. Fernandez-Garcia, E.L. Madruga, A kinetic study on the radical copolymerization of dimethyl itaconate and methyl methacrylate in benzene, *Polymer*, 37 (1996) 263-268.
- [22] E.L. Madruga, M. Fernandez-Garcia, Free-radical homopolymerization and copolymerization of di-n-butyl itaconate, *Polymer*, 35 (1994): 4437-4442.
- [23] M. Fernandez-Garcia, J.L. Fuente, E.L. Madruga, Thermal behavior of poly(dimethyl itaconate) and poly(di-n-butyl itaconate) copolymerized with methyl methacrylate. *Polymer Engineering & Science*, 41 (2001) 1616-1625.
- [24] M. Fernandez-Garcia, E.L. Madruga, Glass transitions in dimethyl and di-n-butyl poly(itaconate ester)s and their copolymers with methyl methacrylate. *Polymer*, 38 (1997) 1367-1371.

- [25] J. Velickovic, S. Vasovic, Kuhn-Mark-Houwink-Sakurada relations and unperturbed dimensions of poly(di-n-alkyl itaconates), *Die Makromolekulare Chemie*, 153 (1972) 207.
- [26] G. Giavaresi, E. B. Minelli, M. Sartori, A. Benini, A. Parrilli, M. C. Maltarello, F. Salamanna, P. Torricelli, R. Giardino, M. Fini, New PMMA-based composites for preparing spacer devices in prosthetic infections, *Journal of Materials Science: Materials in Medicine*, 23 (2012) 1247-1257.
- [27] ISO 20795-1: Dentistry -- Base polymers -- Part 1: Denture base polymers, 2013.
- [28] J. Zheng, Q. Su, C. Wang, G. Cheng, R. Zhu, J. Shi, K. Yao, Synthesis and biological evaluation of PMMA/MMT nanocomposite as denture base material, *Journal of Materials Science: Materials in Medicine*, 22 (2011) 1063-1071.
- [29] J. Crank, *The Mathematics of Diffusion*, Oxford University Press, London, p. 203 (1999).
- [30] W.I. Higuchi, T. Higuchi, Theoretical analysis of diffusional movement through heterogenous barriers, *Journal of the American Pharmaceutical Association. Scientific edition*, 49 (1960) 598-606.
- [31] M.I. Shtilman, *Polymeric Biomaterials*, VSP BV, Utrecht, p. 47, (2003).
- [32] C.Y.K. Lung, B.W. Darvell, Methyl methacrylate monomer-polymer equilibrium in solid polymer, *Dental Materials*, 23 (2007) 88-94.
- [33] P.K. Vallittu, V. Miettinen, P. Alakuijala, Residual monomer content and its release into water from denture base materials, *Dental Materials*, 11 (1995) 338-342.
- [34] K. Shirakawa, Y. Adegawa, S. Yasunami, (Fuji Photo Film Co., Ltd) US 6,773,862, (2004).
- [35] K. Sato, K. Kodama, (Fuji Photo Film Co., Ltd) US 6,777,160 (2004).
- [36] A. Berube, C. Lapalme, (André Berube) US 6,733,125 (2004).
- [37] E. R. Lukenbach, C. Kaminski, S. Pascal-Suisse, M. Tahar, M. Ruggiero, (Johnson & Johnson Consumer Companies, Inc.) US 6,762,158 (2004).
- [38] P. Spasojevic, D. Stamenkovic, R. Pjanovic, N. Boskovic-Vragolovic, J. Dolic, S. Grujic, S. Velickovic, Diffusion and solubility of commercial poly(methyl methacrylate) denture base material modified with dimethyl itaconate and di-n-butyl itaconate during water absorption/desorption cycles, *Polymer International*, 61 (2012) 1272-1278.

- [39] P. Spasojević, V. Panić, S. Šešlija, V. Nikolić, I.G. Popović, S. Veličković, Poly(methyl methacrylate) denture base materials modified with ditetrahydrofurfuryl itaconate: Significant applicative properties. *Journal of the Serbian Chemical Society*, 80 (2015) 1177–1192 .
- [40] Callister, Engennering materials, 7th ed.
- [41] D. Hull and T.W. Clyne, An Introduction to Composite materials, 2nd ed, Cambridge University Press, New York, p47, (1996).
- [42] Handbook of Polymer Applications in Medicine and Medical Devices, 1st Edition, Editors: Modjarrad & Ebnesajjad, Elsevier (2013) ISBN : 9780323228053.
- [43] C. Baudín, Processing of alumina and corresponding composites. In: Ilanes L, Mari D, editors. *Comprehensive Hard Materials. Vol.2. Ceramics*. Amsterdam: Elsevier Ltd.; (2014) 31–72.
- [44] C. Aktas, J. Lee, M.M. Miro, A. Barnoush, M. Veith, Alpha alumina syn-thesis by laser treatment of bi-phasic nanowires, *Applied Surface Science*, 278 (2013) 82-85.
- [45] J. Ma, B. Wu, Effect of surfactants on preparation of nanoscale $\text{-Al}_2\text{O}_3$ powders by oil-in-water microemulsion, *Advanced Powder Technology*, 24 (2013) 354–358.
- [46] T. Shirai, H. Watanabe, M. Fuji, M. Takahashi, Structural properties and surface characteristics on aluminum oxide powders, *Annu Rept Ceram Res Cent Nagoya Institut Technology*, 9 (2009) 23–31.
- [47] S. Cava, S.M. Tebcherani, I.A. Souza, S.A. Pianaro, C.A. Paskocimas, E. Longo, J.A. Varela, Structural characterization of phase transition of Al_2O_3 nanopowders obtained by polymeric precursor method, *Materials Chemistry and Physics*, 103 (2007) 394–399.
- [48] S. Ghanizadeh, X. Bao, B. Vaidhyathan, J. Binner, Synthesis of nano-alumina powders using hydrothermal and precipitation routes: a comparative study, *Ceramics International*, 40 (2014) 1311–1319.
- [49] X. Du, S. Zhao, Y. Liu, J. Li, W. Chen, Y. Cui, Facile synthesis of monodisperse alumina nanoparticles via an isolation-medium-assisted calcination method, *Applied Physics A*, 116 (2014) 1963–1969.

- [50] K.L. Huang, L.G. Yin, S.Q. Liu, C.J. Li, Preparation and formation mechanism of Al₂O₃ nanoparticles by reverse microemulsion, *Transactions of Nonferrous Metals Society of China*, 17 (2007) 633–637.
- [51] J. Li, Y. Pan, C. Xiang, Q. Ge, J. Guo, Low temperature synthesis of ultra-fine-Al₂O₃ powder by a simple aqueous sol–gel process. *Ceramics International*, 32 (2006) 587–591.
- [52] M.R. Karim, M.A. Rahman, M.A.J. Miah, H. Ahmad, M. Yanagisawa, M. Ito, Synthesis of γ -alumina particles and surface characterization, *The Open Colloid Science Journal*, 4 (2011) 32–36.
- [53] A.I.Y. Tok, F.Y.C. Boey, X.L. Zhao, Novel synthesis of Al₂O₃ nano-particles by flame spray pyrolysis. *Journal of Materials Processing Technology*, 178 (2006) 270–273.
- [54] X. Su, S.H. Chen, Z. Zhou, Synthesis and characterization of monodisperse porous γ -Al₂O₃ nanoparticles, *Applied Surface Science*, 258 (2012) 5712–5715.
- [55] T. Noguchi, K. Matsui, N.M. Islam, Y. Hakuta, H. Hayashi, Rapid synthesis of Al₂O₃ nanoparticles in supercritical water by continuous hydrothermal flow reaction system, *The Journal of Supercritical Fluids*, 46 (2008) 129–136.
- [56] K. Laishram, R. Mann, N. Malhan, A novel microwave combustion approach for single step synthesis of Al₂O₃ nanopowders, *Ceramics International*, 38 (2012) 1703–1706.
- [57] M. Nguetack, A.F. Popa, S. Rossignol, C. Kappenstein, Preparation of alumina through a sol–gel process. Synthesis, characterization thermal evolution and model of intermediate boehmite, *Physical Chemistry Chemical Physics*, 5 (2003) 4279–4289.
- [58] F. Mirjalili, H. Mohamad, L. Chuah, Preparation of nano-scale- Al₂O₃ powder by the sol–gel method, *Ceramics Silikaty*, 55 (2011) 378–383.
- [59] Z. Zhang, H. Lei, Preparation of alumina/polymethacrylic acid composite abrasive and its CMP performance on glass substrate, *Microelectronic Engineering*, 85 (2008) 714–720.
- [60] B. Kasprzyk-Hordern, Chemistry of alumina, reactions in aqueous solution and its application in water treatment, *Advances in Colloid and Interface Science*, 110 (2004) 19–48.
- [61] D. Abdelkader, B. Abdecharif, Peculiarity of the cathodoluminescence of α -alumina prepared by calcination of gibbsite powder or generated by oxidation of a metallic

FeCrAl alloy. In: Yamamoto N, editor. *Cathodoluminescence*, Rijeka, Croatia: InTech; (2012) p.209–232.

[62] F.A. Alzarrug, M.M. Dimitrijević, R.M. Jančić Heinemann, V. Radojević, D.B. Stojanović, P.S. Uskoković, R. Aleksić, The use of different alumina fillers for improvement of the mechanical properties of hybrid PMMA composites, *Materials & Design*, 86 (2015) 575-581.

[63] T. Kovačević, J. Rusmirović, N. Tomić, M. Marinović-Cincović, Ž. Kamberović, M. Tomić, A. Marinković, New composites based on waste PET and non-metallic fraction from waste printed circuit boards: Mechanical and thermal properties, *Composites Part B: Engineering*, 127 (2017) 1–14.

[64] ASTM E384 - 16, ASTM E384 - 16 - Stand. Test Method Microindentation Hardness Mater. 201528. (n.d.).

[65] A. Iost, R. Bigot, Hardness of coatings, *Surface and Coatings Technology*, 80 (1996) 117–120.

[66] G. Ali Lazouzi, M. M. Vuksanović, N. Tomić, M. Petrović, P. Spasojević, V. Radojević and R. Jančić Heinemann, Dimethyl itaconate modified PMMA – alumina fillers composites with improved mechanical properties, *Polymer Composites*, (2018), IN PRESS.

[67] S. Ahmed Ben Hasan, M.M. Dimitrijević, A. Kojović, D.B. Stojanović, K. Obradović - Đuričić, R.M. Jančić-Heinemann and R. Aleksić, The effect of alumina nanofillers size and shape on mechanical behavior of PMMA matrix composite, *Journal of the Serbian Chemical Society*, 79 (2014) 1–19.

[68] G. Lazouzi, M.M. Vuksanović, N.Z. Tomić, M. Mitrić, M. Petrović, V. Radojević, R. Jančić Heinemann, Optimized preparation of alumina based fillers for tuning composite properties, *Ceramics International*, 44 (2018) 7442-7449,

[69] R. Jacob, A.P. Jacob, D.E. Mainwaring, Mechanism of the dielectric enhancement in polymer-alumina nano-particle composites, *Journal of Molecular Structure*, 933 (2009) 77–85.

[70] W.X. Zu G, Shen J, Preparation and characterization of monolithic alumina aerogels, *Journal of Non-Crystalline Solids*, 357 (2011) 2903–2906.

- [71] D. Yi Li, Y.S. Lin, Y.C. Li, D.L. Shieh, J.L. Lin, Synthesis of mesoporous pseudo boehmite and alumina templated with 1-hexadecyl-2,3-dimethyl-imidazolium chloride, *Microporous and Mesoporous Materials*, 108 (2008) 276–282.
- [72] G. Zu, J. Shen, X. Wei, Preparation and characterization of monolithic alumina aerogels, *Journal of Non-Crystalline Solids*, 357 (2011) 2903–2906.
- [73] G.V. Franks, Y. Gan, Charging Behavior at the Alumina–Water Interface and Implications for Ceramic Processing, *Journal of the American Ceramic Society*, 90 (2007) 3373-3388.
- [74] T. Shirai, H. Watanabe, M. Fuji, M. Takahashi, Structural properties and surface characteristics on aluminum oxide powders, *Annu Rept Ceram Res Cent Nagoya Institute of Technology*, 9 (2009) 23-31.
- [75] M. Pracella, M.M.U. Haque, V. Alvarez, Compatibilization and properties of EVA copolymers containing surface-functionalized cellulose microfibrils, *Macromolecular Materials and Engineering*, 295 (2010) 949-957.
- [76] G. Socrates, Infrared and Raman Characteristic Group Frequencies, Tables and Charts, John Wiley (2001).
- [77] G. Wypych, Handbook of fillers – Fourth edition, Chem Tec Publishing, Toronto, Canada (2016).
- [78] N. Ilie, T.J. Hilton, S.D. Heintze, R. Hickel, D.C. Watts, N. Silikas, J.W. Stansbury, M. Cadenaro, J.L. Ferracane, Academy of Dental Materials guidance—Resin composites: Part I—Mechanical properties, *Dental materials*, 33 (2017) 880–894.

Прилог 1.

Изјава о ауторству

Потписани-а Gamal Ali Mohamed Lazouzi

број индекса _____

Изјављујем

да је докторска дисертација под насловом

„Sinteza i karakterizacija kompozita sa poboljšanom žilavošću na bazi modifikovanog akrilata i aluminijum-oksidnih čestica za primenu u protetici (Synthesis and characterization of modified acrylate and alumina particles composite with improved toughness for prosthetics application“.

- резултат сопственог истраживачког рада,
- да предложена дисертација у целини ни у деловима није била предложена за добијање било које дипломе према студијским програмима других високошколских установа,
- да су резултати коректно наведени и
- да нисам кршио/ла ауторска права и користио интелектуалну својину других лица.

Потпис докторанда

У Београду, 25.6.2017

_____ 

Прилог 2.

Изјава о истоветности штампане и електронске верзије докторског рада

Име и презиме аутора Gamal Ali Mohamed Lazouzi _____

Број индекса _____

Студијски програм инжењерство материјала _____

Наслов рада „Sinteza i karakterizacija kompozita sa poboljšanom žilavošću na bazi modifikovanog akrilata i aluminijum-oksidnih čestica za primenu u protetici (Synthesis and characterization of modified acrylate and alumina particles composite with improved toughness for prosthetics application“.

Ментор Радмила Јанчић Хајнеман _____

Потписани/а _____

Изјављујем да је штампана верзија мог докторског рада истоветна електронској верзији коју сам предао/ла за објављивање на порталу **Дигиталног репозиторијума Универзитета у Београду**.

Дозвољавам да се објаве моји лични подаци везани за добијање академског звања доктора наука, као што су име и презиме, година и место рођења и датум одбране рада.

Ови лични подаци могу се објавити на мрежним страницама дигиталне библиотеке, у електронском каталогу и у публикацијама Универзитета у Београду.

Потпис докторанда

У Београду, 25.06.2018 _____



Прилог 3.

Изјава о коришћењу

Овлашћујем Универзитетску библиотеку „Светозар Марковић“ да у Дигитални репозиторијум Универзитета у Београду унесе моју докторску дисертацију под насловом:

„Sinteza i karakterizacija kompozita sa poboljšanom žilavošću na bazi modifikovanog akrilata i aluminijum-oksidnih čestica za primenu u protetici (Synthesis and characterization of modified acrylate and alumina particles composite with improved toughness for prosthetics application“.

која је моје ауторско дело.

Дисертацију са свим прилозима предао/ла сам у електронском формату погодном за трајно архивирање.

Моју докторску дисертацију похрањену у Дигитални репозиторијум Универзитета у Београду могу да користе сви који поштују одредбе садржане у одабраном типу лиценце Креативне заједнице (Creative Commons) за коју сам се одлучио/ла.

1. Ауторство
2. Ауторство - некомерцијално
3. Ауторство – некомерцијално – без прераде
4. Ауторство – некомерцијално – делити под истим условима
5. Ауторство – без прераде
6. Ауторство – делити под истим условима

(Молимо да заокружите само једну од шест понуђених лиценци, кратак опис лиценци дат је на полеђини листа).

Потпис докторанда

У Београду, 25.06.2018 _____

_____ 

1. Ауторство - Дозвољавање умножавање, дистрибуцију и јавно саопштавање дела, и прераде, ако се наведе име аутора на начин одређен од стране аутора или даваоца лиценце, чак и у комерцијалне сврхе. Ово је најслободнија од свих лиценци.

2. Ауторство – некомерцијално. Дозвољавање умножавање, дистрибуцију и јавно саопштавање дела, и прераде, ако се наведе име аутора на начин одређен од стране аутора или даваоца лиценце. Ова лиценца не дозвољава комерцијалну употребу дела.

3. Ауторство - некомерцијално – без прераде. Дозвољавање умножавање, дистрибуцију и јавно саопштавање дела, без промена, преобликовања или употребе дела у свом делу, ако се наведе име аутора на начин одређен од стране аутора или даваоца лиценце. Ова лиценца не дозвољава комерцијалну употребу дела. У односу на све остале лиценце, овом лиценцом се ограничава највећи обим права коришћења дела.

4. Ауторство - некомерцијално – делити под истим условима. Дозвољавање умножавање, дистрибуцију и јавно саопштавање дела, и прераде, ако се наведе име аутора на начин одређен од стране аутора или даваоца лиценце и ако се прерада дистрибуира под истом или сличном лиценцом. Ова лиценца не дозвољава комерцијалну употребу дела и прерада.

5. Ауторство – без прераде. Дозвољавање умножавање, дистрибуцију и јавно саопштавање дела, без промена, преобликовања или употребе дела у свом делу, ако се наведе име аутора на начин одређен од стране аутора или даваоца лиценце. Ова лиценца дозвољава комерцијалну употребу дела.

6. Ауторство - делити под истим условима. Дозвољавање умножавање, дистрибуцију и јавно саопштавање дела, и прераде, ако се наведе име аутора на начин одређен од стране аутора или даваоца лиценце и ако се прерада дистрибуира под истом или сличном лиценцом. Ова лиценца дозвољава комерцијалну употребу дела и прерада. Слична је софтверским лиценцама, односно лиценцама отвореног кода.

CV of the candidate

Gamal Ali Mohamed Lazouzi master engineer of technology was born on 2nd of June 1982. In Bani Waleed, Libya. Elementary school and high school he completed in his birth place. Faculty of Medical Technology he finished in Misurata, Libya. He enrolled to master studies at the Faculty of Technology and Metallurgy in 2011 and he completed master studies in 2012. obtaining the degree of Master engineer of technology.

In 2012. The candidate enrolled to doctoral studies at the Faculty of Technology and Metallurgy in University of Belgrade and passed all exams according to the program with success.

Biografija kandidata

Kandidat Gamal Ali Mohamed Lazouzi master inženjer tehnologije rođen je 02.06.1982. godine u Bani Waleed, Libija. Osnovnu i srednju školu, završio je u rodnom mestu. Fakultet za medicinsku tehnologiju završio je u Misurati, Libija. Master studije na Tehnološkom fakultetu u Beogradu upisao je 2011. godine, a završio je na istom fakultetu 2012. i stekao zvanje master diplomirani inženjer tehnologije za inženjerstvo materijala.

Na Katedri za Konstrukcije materijale na Tehnološko-metalurškom fakultetu Univerziteta u Beogradu upisao je doktorske studije 2012. godine i sve ispite po nastavnom planu i programu položio je sa uspehom.

Nakon završetka osnovnih studija, zaposlen je kao asistent u nastavi na Fakultetu za dentalnu tehnologiju u Bani Waleedu, Libija.